LBL-10009

Lawrence Berkeley Laboratory
UNIVERSITY OF CALIFORNIA

Materials & Molecular
Research Division

MULTIPHOTON ASSOCIATION OF POLYATOMIC MOLECULES

Peter A. Schulz
(Ph. D. thesis)

October 1979

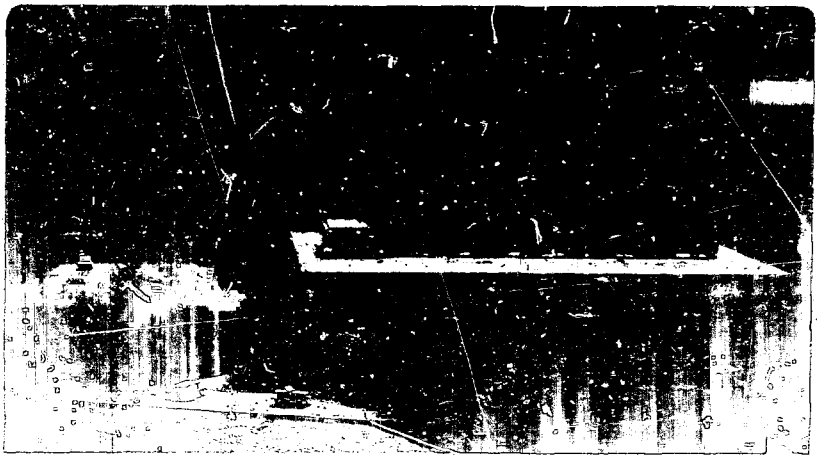

Prepared for the U.S. Department of Energy under Contract W-7405-ENG-48

LBL-10009

MULTIPHOTON DISSOCIATION OF POLYATOMIC MOLECULES

Peter A. Schulz

Materials and Molecular Research Division
Lawrence Berkeley Laboratory

and

Department of Physics
University of California
Berkeley, California 94720

OCTOBER 1979

ABSTRACT

The dynamics of infrared multiphoton excitation and dissociation of SF_6 has been investigated under collision free conditions by a crossed laser-molecular beam method. In order to understand the excitation mechanism and to elucidate the requirements of laser intensity and energy fluence, a series of experiments have been carried out to measure the dissociation yield dependences on energy fluence, vibrational temperature of SF_6, the pulse duration of the CO_2 laser and the frequency in both one and two laser experiments. Translational energy distributions of the SF_5 dissociation product measured by time of flight and angular distributions and the dissociation lifetime of excited SF_6 as inferred from the observation of secondary dissociation of SF_5 into SF_4 and F during the laser pulse suggest that the dynamics of dissociation of excited

molecules is dominated by complete energy randomization and rapid intramolecular energy transfer on a nanosecond timescale, and can be adequately described by RRKM theory.

An improved phenomenological model including the initial intensity dependent excitation, a rate equation describing the absorption and stimulated emission of single photons, and the unimolecular dissociation of excited molecules is constructed based on available experimental results. The model shows that the energy fluence of the laser determines the excitation of molecules in the quasi-continuum and the excess energy with which molecules dissociate after the laser pulse. The role played by the laser intensity in multiphoton dissociation is more significant than just that of overcoming the intensity dependent absorption in the lowest levels. Once molecules are excited to energies where the rate of decomposition competes with the rate of up-excitation, the average level of excitation of the dissociating molecules is determined by the laser intensity. A comparison between the model calculations for SF_6 and CF_3I shows that the much larger CF_3I dissociation rate constant at the same level of excess excitation causes CF_3I to dissociate immediately after exceeding the dissociation energy, in contrast to the absorption by SF_6 of many photons in excess of that required for dissociation.

D E D I C A T I O N

This work is dedicated to the memory of my father who infused me with the desire to understand the interactions of atoms and molecules with each other and with other particles. Specifically, he first brought to my attention the problem of multiphoton dissociation of polyatomic molecules. It is my hope that this thesis would have answered his questions, though, undoubtedly, he would have posed still more questions that cannot yet be answered.

ACKNOWLEDGEMENTS

Large parts of this work were done in collaboration with others. My collaborators generously gave their time in order that we could understand multiphoton dissociation of polyatomic molecules.

Yuan Lee is the person most responsible for the success of the experiments that culminated in this thesis. When I did not know what part of the molecular beam apparatus had gone awry, Yuan was there to help find and fix the problem. I most appreciate his incessant search for experimental results, his quick comprehension and analysis of those results, and his synthesis of a new framework in which to view the experimental results.

Ron Shen was also intimately involved in these experiments and I thank him for giving me a clearer understanding of the excitation process in multiphoton dissociation. By his patience in pointing out how my explanations were confused and muddled, he helped to make this thesis into as readable a document as it is. I owe him a debt of gratitude for making me a better writer.

Mike Coggiola first introduced me to the crossed molecular beam technology that was vital for doing these experiments. Together with Ed Grant, we made the first tentative steps toward understanding SF_6 multiphoton dissociation, which is the subject of Chapter II. Ed Grant performed many calculations that convinced me of the importance of the rate equation model for understanding the roles of laser intensity and energy fluence in multiphoton dissociation, the subject of Chapter III.

Aasmund Sudbø is primarily responsible for much of the analysis of the many angular and time-of-flight distributions that we obtained during 1977. He combined the traits of efficiency and diligence at work with a good sense of humor. Happily these traits were also apparent in Doug Krajnovich during our search to unravel the mysteries of C_2F_5Cl multiphoton dissociation. Anna Giardini-Guidoni provided pleasant and valuable assistance during three months of study of C_2F_5Cl.

I wish to thank Ann Weightman for her essentially error free typing of innumerable numbers of edited and re-edited manuscripts. Alan Susoeff provided the technical support that allowed us to quickly proceed to the next experiment.

This work was supported by the Division of Advanced Systems Materials Productions, Office of Advanced Isotope Separation, U.S. Department of Energy under contract No. W-7405-Eng-48.

My most heartfelt appreciation is for my friends in the Yuan Lee group, my friends from M.I.T., and my mother and brother, all of whom supported my efforts to overcome the trials and tribulations during four years at Berkeley.

MULTIPHOTON DISSOCIATION OF POLYATOMIC MOLECULES

Contents

I. INTRODUCTION

The study of vibrational excitation of molecules by radiation has been an ongoing pursuit for approximately 50 years. The quantization of molecular vibrations and the infrared excitation of diatomic molecules by a single photon was understood in the 1930's. Since then, advances have been made in the theoretical understanding of larger polyatomic molecules. With the comparatively recent development of high power infrared lasers, the much more complicated problems of multiphoton excitation and dissociation of polyatomic molecules have been studied.

The possibility that a polyatomic molecule placed in the intense field of an infrared laser can absorb enough photons to dissociate was first suggested by Isenor and Richardson[1] in 1971 based on their experimental observation of luminescence from dissociation products. In 1973 Isenor et al.[2] and Letokhov et al.[3,4] discovered that the luminescence contained an instantaneous and a delayed component; the instantaneous component suggesting that the absorption of many photons and the subsequent molecular dissociation could take place under isolated collision-free conditions. This infrared multiphoton dissociation process was subsequently shown to be isotopically selective in 1974 by Ambartzumian et al.[5,6] and Lyman et al.[7] High efficiency and high selectivity of the process, as manifested by separation of isotopes, gave tremendous impetus to a rapid growth in this new area of research.

Actually , a considerably amount of interest and excitement was also generated by the suggestion that multiphoton excitation is a novel method for energizing molecules, one that offered the potential for vibrational mode control of molecular decomposition. In other words, by depositing energy into particular vibrational modes, it was hoped that molecules would dissociate along certain reaction pathways different from those of thermal decomposition. Initial experimental results appeared to support this hypothesis. The first reported primary product analysis for the multiphoton dissociation of SF_6[8] indicated that this molecule dissociated into SF_4 and F_2, bypassing the lower energy SF_5 and F fragmentation channel. Results of gas cell experiments with $CFCl_3$ were interpreted to evidence direct dissociation into CFCl and Cl_2.[9] However, molecular beam experiments show that these conclusions are incorrect. In multiphoton dissociation of molecular beams of SF_6 and $CFCl_3$ collisionless production of SF_4 and CFCl, respectively, has been observed. However, these products are a consequence of multiphoton dissociation of the primary products SF_5 and $CFCl_2$;[10,11] not of a mode selective decomposition as originally hypothesized.

The question of whether any multiphoton dissociation involves a mode selective decomposition is only one of the many questions that I have tried to answer using the molecular beam technique. One of the most fundamental questions is whether multiphoton excitation and dissociation can take place in a collision-free environment. The

success of the molecular beam experiments shows that a truly collisionless multiphoton dissociation occurs. In addition, questions on the identity of the primary dissociation products and the dissociation dynamics could be and were answered by molecular beam as well as other techniques.[11-18] Other questions concerning the effects of the internal temperature of the polyatomic molecule, the laser pulse duration, the laser energy fluence, and the laser frequency on the multiphoton dissociation could also be answered by collisionless molecular beam experiments, whereas collisions often made the analogous gas cell experimental results difficult or impossible to interpret. Questions such as (1) what is the population distribution of molecules after illumination by a high power infrared laser and (2) is the energy in the molecule randomized among the vibrational modes of the molecule cannot be answered directly, but require the synthesis of a model whose validity must be tested by comparison with experimental results.

A successful qualitative model has been constructed based on the experimental results. A polyatomic molecule with little internal energy has discrete states, so monochromatic laser radiation can selectively excite a particular vibrational mode of the molecule. Indeed the monochromatic excitation over the discrete states is responsible for the isotopic selectivity of multiphoton dissociation. With increasing internal energy in the molecule the density of states increases and the vibrational states soon form a quasi-continuum.[2,19,20]

This precludes the possbility of a mode selective decomposition unless a single eigenstate or a coherent superposition of eigenstates is excited. Excitation through the quasi-continuum occurs via non-isotope selective, resonant stepwise transitions to and beyond the dissociation energy. Beyond the dissociation energy, decomposition occurs after the excitation energy is randomized in the moelcule. The translational energy distribution of the products produced in multiphoton dissociation is consistent with the energy randomization hypothesis for a wide variety of molecules studied in molecular beam experiments.[11,12]

Further molecular beam experiments as well as other types of experiments gave more support for the model and led to the construction of a simple, quantitative rate equation model for multiphoton dissociation experiments on a nanosecond time scale.[21,22] The model includes an intensity dependent excitation over the discrete states, a quasi-continuum where the energy fluence, not the laser intensity, determines the amount of excitation, and for molecules with internal energies greater than the dissociation energy, a dissociation which occurs at a rate given by the RRKM (statistical) theory of unimolecular decomposition. One of the most important features of the model is that when molecules are excited far enough, the dissociation rate competes with the up-excitation rate. The internal energy that molecules have when they dissociate, which determines the possible dissociation products, is then controlled by the laser intensity.

Thus, experiments on molecules showing that the dissociation products depend on the laser intensity,[23] which have been used to defend the mode selective decomposition hypothesis, are actually a natural consequence of the rate equation model.

In this thesis I concentrate on the rate equation model for SF_6 and the molecular beam experiments on SF_6 multiphoton dissociation which can be used to test the rate equation model. The interpretation of the molecular beam results, essential to testing the rate equation model, relies on an understanding of the experimental apparatus. Therefore, the crossed CO_2 laser-SF_6 molecular beam apparatus used in the experiments is described in Chapter II except for two features: (1) the triple differential pumping of the moelcular beam source and (2) the ion fragmentation of netural molecules by electron bombardment ionization, which are discussed in Appendix B. The results of the molecular beam experiments and the results of Black et al.[24] are then used to construct and justify a rate equation model for SF_6 multiphoton dissociation in Chapter II. The role intensity and energy fluence play in the multiphoton excitation and dissociation is explained in Chapter III using the rate equation model. The computer program used for the model calculations is given in Appendix C.

REFERENCES

1. N. R. Isenor and M. C. Richardson, Appl. Phys. Lett. 18, 224 (1971).

2. N. R. Isenor, V. Merchant, R. S. Hallsworth, and M. C. Richardson, Can. J. Phys. 51, 1281 (1973).

3. V. S. Letokhov, E. A. Ryabov, and O. A. Tumanov, Opt. Commun. 5, 168 (1972).

4. V. S. Letokhov, E. A. Ryabov, and O. A. Tumanov, Sov. Phys. JETP 36, 1069 (1973).

5. R. V. Ambartzumian, V. S. Letokhov, E. A. Ryabov, and N. V. Chekalin, JETP Lett. 20, 273 (1974); R. V. Ambartzumian, Yu. A. Gorokhov, V. S. Letokhov, and G. N. Makarov, JETP Lett. 21, 171 (1974).

6. R. V. Ambartzumian, Yu. A. Gorokhov, V. S. Letokhov, and G. N. Makarov, JETP Lett. 22, 43 (1975).

7. J. L. Lyman, R. J. Jensen, J. Rink, C. P. Robinson, and S. D. Rockwood, Appl. Phys. Lett. 27, 87 (1975).

8. K. C. Kompa in Tunable Lasers and Applications, ed., A. Moordian, T. Jaeger, P. Stokseth (Berlin, Springer, 1976), p.177.

9. D. F. Dever and E. Grunwald, J. Am. Chem. Soc. 98, 5055 (1976).

10. E. R. Grant, M. J. Coggiola, Y. T. Lee, P. A. Schulz, Aa. S. Sudbø, and Y. R. Shen, Chem. Phys. Lett. 52, 595 (1977).

11. Aa. S. Sudbø, P. A. Schulz, E. R. Grant, Y. R. Shen, and Y. T. Lee, J. Chem. Phys. 70, 912 (1979).

12. M. J. Coggiola, P. A. Schulz, Y. T. Lee, and Y. R. Shen, Phys. Rev. Lett. 38, 17 (1977).

13. Aa. S. Sudbø, P. A. Schulz, Y. R. Shen, and Y. T. Lee, J. Chem. Phys. 69, 2312 (1978).

14. D. S. King and J. C. Stephenson, Chem. Phys. Lett. 51, 48 (1977).

15. J. C. Stephenson and D. S. King, J. Chem. Phys. 69, 1485 (1978).

16. J. D. Campbell, M. H. Yu, M. Mangir, and C. Wittig, J. Chem. Phys. 68, 3854 (1978).

17. C. R. Quick, Jr. and C. Wittig, Chem. Phys. Lett. 48, 420 (1977); also in Chem. Phys. 32, 75 (1978).

18. M. L. Lesiecki and W. A. Guillory, J. Chem. Phys. 66, 4239 (1977).

19. N. Bloembergen, Opt. Commun. 15, 416 (1975).

20. V. M. Akulin, S. S. Alimipiev, N. V. Karlov, and L. A. Shelepin, Sov. Phys. JETP 42, 427 (1975).

21. E. R. Grant, P. A. Schulz, Aa. S. Sudbø, Y. R. Shen, and Y. T. Lee, Phys. Rev. Lett. 40, 115 (1978).

22. J. L. Lyman, J. Chem. Phys. 67, 1868 (1977).

23. D. M. Brenner, Chem. Phys. Lett. 57, 357 (1978).

24. J. G. Black, P. Kolodner, M. J. Schultz, E. Yablonovitch, and N. Bloembergen, Phys. Rev. A 19, 704 (1979).

II. MULTIPHOTON DISSOCIATION OF SF_6 BY A MOLECULAR BEAM METHOD

INTRODUCTION

In recent years, a considerable amount of research activity has been directed toward understanding the phenomenon of infrared multiphoton dissociation (MPD) of molecules.[1-4] Sulfur hexafluoride has figured prominently in much of this research. It was among the first molecules to be dissociated by a high power CO_2 laser. Pressure dependence of isotopic selectivity in the MPD of SF_6[2-4] suggested that the dissociation took place under collisionless conditions. Later, molecular beam expeirments confirmed this phypothesis.[5,6]

Early studies on the MPD products of SF_6 were interpreted to indicate (1) dissociation to SF_4 and F_2,[3,5] bypassing the lower energy SF_5 + F fragmentation channel and (2) absorption of 80 to 90 photons before dissociation.[7] These results led to the theoretical construction of coherent, mode-specific models for vibrational excitation in intense laser fields. More recent experiments, including the ones reported here, have shown that the primary dissociation occurs via a S-F bond scission.[6,8-11] The translational energy distributions of the fragments seem to imply that the excitation energy is completely randomized before decomposition. Experimental limits placed on the lifetime for decomposition[11] and a recent measurement of the total number of photons absorbed before decomposition[12] are in agreement with the assumption of randomization of the vibrational energy within the molecule. Lyman and Rockwood[13] and Black et al.[14] found that the energy fluence, not the intensity,

determines the dissociation yield. Simple, incoherent sequential excitation models have been found to fit much of the data.[15,16]

The well-accepted, qualitative model for MPD of SF_6 involves, first, a near-resonant absorption of 3-6 infrared photons in a single vibrational ladder. Anharmonicity causes a mismatch between the vibrational spacing and the laser frequency which is nearly compensated by mechanisms such as allowed rotational transitions. At higher energy the density of states becomes large, and intermode coupling is strong so that the energy states of the molecules form a quasi-continuum. Further excitation of the molecules through this quasi-continuum occurs via resonant stepwise single-photon absorption. Eventually, the molecules are excited beyond the dissociation energy and dissociate. Because the energy is completely randomized in the SF_6 molecule, the dissociation can be described by a standard statistical theory of unimolecular reactions such as the RRKM theory. Statistical theory predicts that dissociation rates increase rapidly with increasing excess energy (i.e., excitation energy minus the dissociation energy) in the molecule and soon dissociation of the molecules starts to compete with up-excitation of the molecules by the laser. Hence, when the energy fluence of the laser is sufficiently high, most of the molecules will dissociate from excitation levels where the dissociation rate is roughly equal to the upexcitation rate.

MPD experiments performed on SF_6 in a molecular beam apparatus have provided a large body of information useful in elucidating the

details of the MPD of SF_6. Measurements of the angular and time-of-flight distributions of the products, which have been reported previously,[6,10,11] probe the dynamics of dissociation. In order to provide a more complete picture of MPD of SF_6, we have extended our studies to investigate the dependence of the MPD yield on the amount of internal excitation in SF_6. The absorption of photons by SF_6 depends upon the frequency and power of the infrared radiation as has been observed in many previous experiments (see Ref. 1). By performing the experiments in a molecular beam apparatus, we have been able to obtain information that is not available in a gas cell experiment. In particular, the vibrational temperature of SF_6 in a molecular beam has been varied while keeping the rotational temperature relatively low in order to study the absorption under different initial conditions. These new results in conjunction with earlier results enable us to produce a more realistic model to describe the MPD of SF_6.

EXPERIMENTAL

Our experiments were carried out by a molecular beam method in which a collimated molecular beam with a narrow well-defined velocity distribution was crossed by a pulsed CO_2 laser beam. The fragments resulting from MPD of the beam were detected as a function of angle by a rotatable quadrupole mass spectrometer with an electron bombardment ionizer. The direct identification of primary dissociation fragments and the measurements of their velocity and angular distributions under various experimental conditions were the basis for deriving information on the dynamics of MPD of SF_6.

The molecular beam of SF_6 was formed by expansion of neat SF_6 typically from 150 torr through a 0.1 mm diameter quartz nozzle. The average velocity of the SF_6 beam was 3.25×10^4 cm/sec and the velocity spread could be characterized by a speed to width ratio of $v/\Delta v = 4$ where Δv is the FWHM velocity spread. Three stages of differential pumping were used to obtain a well-defined beam of 2 mm diameter and $\sim 1^o$ FWHM angular spread. The SF_6 beam density at the point where it crossed with the CO_2 laser was estimated to be 10^{-5} torr, compared with a total background pressure of 5×10^{-7} torr.

The internal translational temperature of SF_6 in the molecular beam was measured from the FWHM velocity spread of the beam to be $T_r \sim 20K$. In the expansion, the rotational (R) and vibrational (V) temperatures of SF_6 may be different from the internal translational temperature of the beam. Lambert et al.[17] measured that 1005 collisions are required to cool SF_6 by V → T energy transfer. This was approximately 25 times the number of collisions that occured in the expansion.

Therefore the internal vibrational temperature of SF_6 in the beam was very close to the temperature of SF_6 prior to the expansion. The rotational temperature of SF_6 in the beam could be measured from the average translational energy of the beam that depends on the initial pressure. In the isenthalpic expansion to form the molecular beam, the translational energy of the beam should be:

$$E_{tr} = kT + \frac{3}{2} k(T-T_t) + \frac{3}{2} k(T-T_r)$$

The initial temperature prior to expansion, T, was 300K. Therefore, the rotational temperature, T_r, was approximately 150K after the expansion. By cooling and heating the nozzle, the influence of vibrational temperature on MPD of SF_6 was studied. Cooling and heating the nozzle may affect the rotational temperature of SF_6 in the beam to some extent, but the rotational temperature was lower than the vibrational temperature and thus was subject to smaller temperature changes. Nozzle temperatures of up to 500 K were achieved by a simple electrical heater wound around the nozzle. A liquid nitrogen cooled arm thermally connected to the nozzle was used to cool the SF_6 down to 210 K prior to expansion.

The interaction region was defined by the intersection of the molecular beam and the partially focused output of a grating tuned CO_2 laser. The CO_2 laser, a Tachisto 215G, delivered a 2 Joule pulse in a 60 ns FWHM spike followed by a 600 ns tail. The tail contained about 40% of the total energy. For certain experiments the temporal characteristics of the laser pulse were modified. A shorter laser pulse duration was obtained using a discharge shutter consisting of two 13 cm focal length ZnSe lenses placed 26 cm apart. These produced

air breakdown on the leading edge of the pulse and provided a truncated output of about 15 ns FWHM with no tail. The laser pulse was then focused into the scattering chamber by a 25 cm focal length ZnSe lens. The laser pulse energy entering the interaction region was adjusted using external attenuators. The cross sectional area of the laser beam in the interaction region could be controlled by adjusting the position of the lens to vary the distance from the focal point to the interaction region. The energy fluence was then determined by a measurement of the laser energy and the area of the laser beam in the interaction region. The energy fluence fluctuation was less than 50% including spatial and pulse to pulse variations. A slanted pyrex dish was used after the interaction region in the vacuum chamber to absorb the 10μ radiation to prevent photodesorption of adsorbed molecules from the surface of the stainless steel chamber. Elastic scattering of SF_6 from the desorbed particles was a source of contamination in Ref. 6.

In order to investigate the absorption process in more detail, MPD of SF_6 was also carried out with two Tachisto 215G CO_2 lasers operating at two different frequencies. One laser excited SF_6 up the discrete vibrational ladder to the quasi-continuum and the other provided sufficient energy fluence to decompose the SF_6 molecules in the quasi-continuum. The second laser was tuned to a frequency which was not absorbed by cold SF_6. In this way the quasi-continuum absorption could be studied separately from the initial 3-6 photon absorption.

The fragments from the interaction region were monitored by the rotatable detector which has been described previously.[18] Briefly, a set of 3 mm x 3 mm collimating slits on the walls of the triply

differentially pumped detector insured an angular resolution of 1^0 (0.5 millisteradian solid angle). The innermost region at a pressure of less than 10^{-10} torr contained a 200 eV coaxial electron bombardment ionizer of the Brinks type. The ionized molecular fragments were focused and analyzed by a quadrupole mass filter. The ions were counted using a Daly type scintillation ion counter. A typical background count rate for the SF_3^+ ion with the SF_6 molecular beam on was 10^5 counts/sec at 5^0 away from the beam.

The electronics setup for data collection is shown schematically in Fig. 1. The laser(s) was fired at a rate of 0.7 Hz by a pulse generator. For the measurement of angular distributions the pulse generator was also used to trigger two gates. One gate enabled the first channel of a dual channel scaler after an initial delay that allowed the fragments to arrive at the detector. The scaler accumulated signal from the detector's ion counter for a gate width corresponding to the width of the flight time distribution (around 0.8 ms). Then after a second delay of 10 ms the other channel of the scaler was enabled by the second gate to count background for the same gate width time.

Velocity distributions of the fragments were measured by the time-of-flight method using a multichannel scaler (either a Hewlett-Packard 5422B Digital Processor or a 256-channel scaler interfaced with a Nova 1220 minicomputer). The trigger pulse for the laser was also used to start the time sweep for the multichannel scaler. The delay between the trigger for the laser and the laser pulse was measured by a photon drag detector to be less than 1 μs. This delay was

Fig. 1. Electronics schematic of the two laser experiment. Many of the experiments were run with just one laser operating.

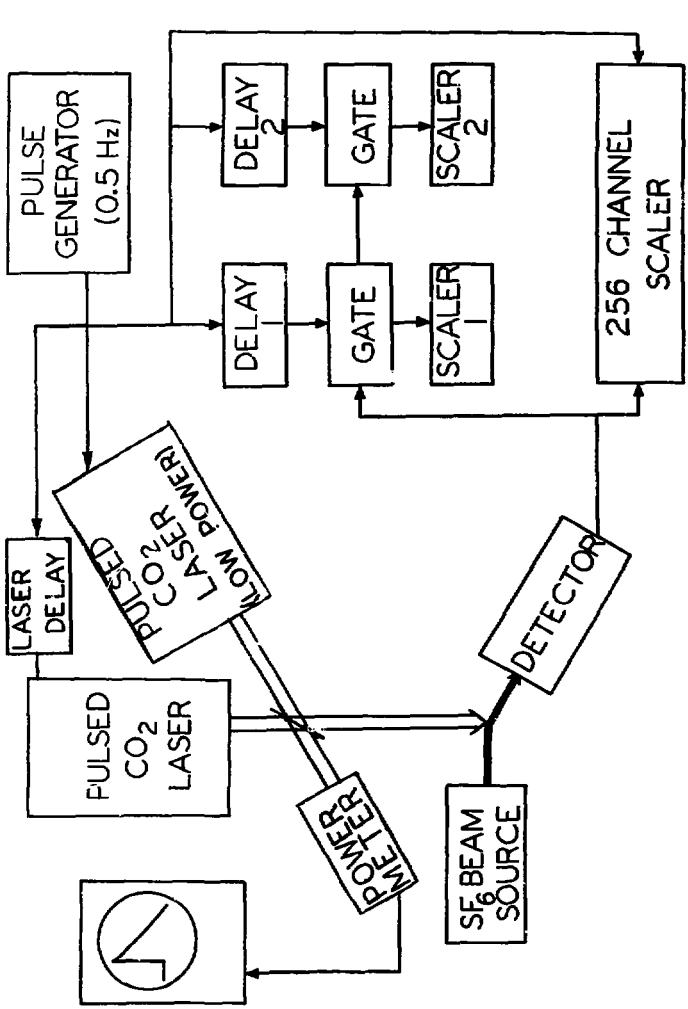
PULSE GENERATOR (0.5 Hz)
DELAY 2
GATE
SCALER 2
DELAY 1
GATE
SCALER 1
256 CHANNEL SCALER
LASER DELAY
PULSED CO2 LASER (LOW POWER)
PULSED CO2 LASER
POWER METER
DETECTOR
SF6 BEAM SOURCE
XBL 768-10159 A

Fig. 1

unimportant because the fastest flight time of sulfur containing fragments was more than 200 μs and the dwell time per channel was typically 10 μs. The time-of-flight spectrum was taken in 250 channels, which was long enough to collect the signal and to determine the baseline of background accurately.

RESULTS AND ANALYSIS

The first objective of this series of experiments is to determine the MPD products of SF_6. Some of these results have been reported previously[11] but are included here for completeness. SF_3^+ and SF_2^+ are the major ion fragments observed in the ionizer from the neutral molecular fragments of SF_6 under MPD. Time-of-flight spectra and angular distributions of SF_3^+ and SF_2^+ are identical, with a signal ratio $SF_3^+:SF_2^+$ of $4.5 \pm 0.5:1$ when using a 5 J/cm^2 CO_2 laser pulse tuned to 944 cm^{-1} (see Fig. 2). The $SF_3^+:SF_2^+$ ion fragmentation ratio from SF_4 is measured to be 2.2:1 using 200 eV electrons. We expect that the $SF_3^+:SF_2^+$ ratio produced in the ionizer for SF_5 should be greater than the ratio observed for SF_4. The observed ratio of $SF_3^+:SF_2^+$ and the identical angular and velocity distributions of SF_3^+ and SF_2^+ are therefore indicative of SF_5, not SF_4, as the major product from MPD of SF_6. The possibility that the signal might arise from SF_6 entering the detector can also be ruled out since the SF_5^+ and SF_4^+ signals expected from the electron impact fragmentation of SF_6 were not observed. Thus, we conclude that in our experiment, at moderately low laser fluence (< 8 J/cm^2), MPD of SF_6 yields predominantly the products SF_5 and F.

When the energy fluence of the CO_2 laser pulse at 944 cm^{-1} is increased to 15 J/cm^2, the angular distributions of the SF_3^+ and SF_2^+ ion fragments (see Fig. 2) differ from each other, indicating the presence of additional neutral fragments from MPD. The $SF_3^+:SF_2^+$ signal ratio changes from about 4:1 at 5^0 to 2.5:1 at 30^0 from the SF_5 beam. The $SF_3^+:SF_2^+$ ratio at large angles is indicative of the appearance of a secondary product, namely, SF_4. One might think that

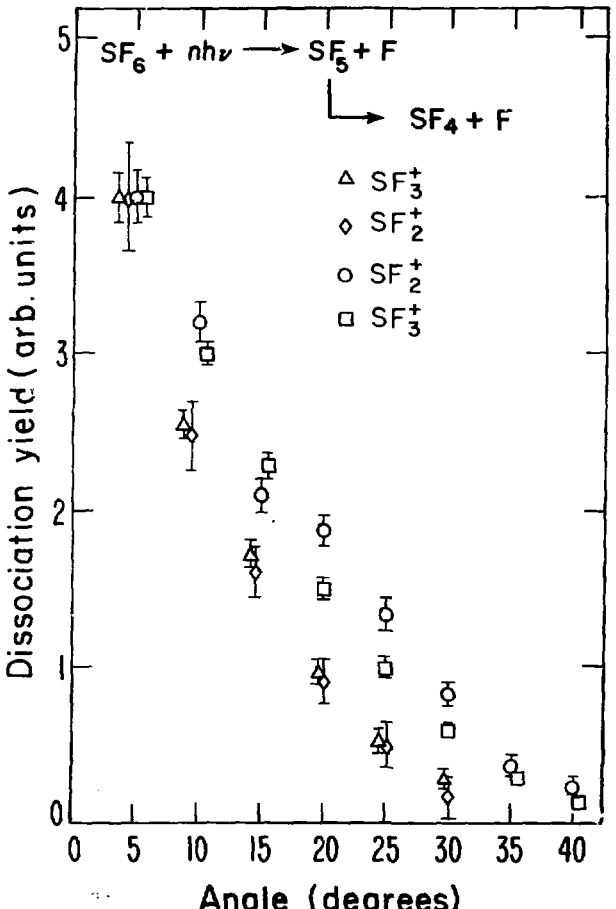

XBL798-2389

Fig. 2. Angular distributions of SF_3^+ and SF_2^+ signals at high and low laser intensity. At high laser intensity a secondary dissociation occurs.

the change in the $SF_3^+:SF_2^+$ ratio is caused by an increase in internal excitation of the SF_5 fragment from MPD of SF_6. At increased laser power, SF_6 is excited to higher energy before dissociating, producing SF_5 which also has higher internal excitation. If this is true, then the $SF_3^+:SF_2^+$ ratio would change continuously with the energy fluence, but be nearly independent of the angle. However, the observations in this experiment are that the $SF_3^+:SF_2^+$ ratio changes dramatically with angle, and also rapidly with energy fluence, from 4.5:1 at 5 J/cm^2 to 2:1 at 20 J/cm^2. The hypothesis that SF_4 and F_2 may be the products of SF_6 MPD competing with dissociation into SF_5 and F is also inconsistent with this experiment. First, no F_2^+ is observed in the mass spectrometer. Second, dissociation of SF_6 into SF_4 and F_2 is likely to have an energy barrier in the exit channel that should lead to a very broad angular distribution of the fragments as has been observed in other three center elimination reactions.[19] Such an angular distribution is not observed. Therefore, we conclude that at high energy fluence SF_5, formed by MPD of SF_6, absorbs 944 cm^{-1} laser radiation and dissociates into SF_4 and F.

Some of our most significant findings concerning the dynamics of MPD are contained in our angular and velocity distributions. After changing the laser polarization, no change is observed in the angular or time-of-flight distributions. This indicates that the velocity distribution of fragments in the center of mass frame is isotropic. The transformation of an isotropic product center of mass translational energy distribution to laboratory angular and velocity distributions for multiphoton dissociation has been discussed in detail elsewhere.[19]

Figure 3 shows the theoretical and experimental velocity distributions of SF_5 detected as SF_3^+ produced by a laser energy fluence of 5 J/cm^2. The theoretical curves were calculated from the translational energy distributions shown in Fig. 4. The energy distributions were derived from the RRKM statistical theory of unimolecular dissociation. The RRKM theory only predicts the dissociation rate constant and the translational energy distribution of the fragments in the critical configuration. However, for loose complexes[19,20] the absence of barriers in the exit channel makes the translational energy distribution of the fragments in the critical configuration essentially the same as the final translational energy distribution of the fragments. The theory assumes that a molecule excited above the dissociation level randomly samples the available vibrational phase space in the process of decomposition. The agreement between theory and experiment on the translational energy distributions strongly supports this assumption. Many accounts have already been given of the RRKM theory and the calculation of dissociation rate constants[11,16,20,21] and will not be repeated here. However it should be pointed out that a discrepancy which appeared in the literature on the dissociation rate constants for SF_6 has now been resolved. The previous results of this group[11] gave significantly higher rate constants than Lyman's calculations[16] because we used a dissociation energy of D = 77 kcal/mole rather than the dissociation energy of D = 93 kcal/mole.[16] The results of our RRKM calculation using D = 93 kcal/mole agree with the results reported in Ref. 16 (see Appendix).

Fig. 3. Velocity distribution of SF_3^+ compared with three RRKM predicted velocity distributions. The vertical axis plots the number density of fragments normalized to the observed angular distribution.

--- — — — 5 excess photons

— — — — 8 excess photons

———————— 12 excess photons

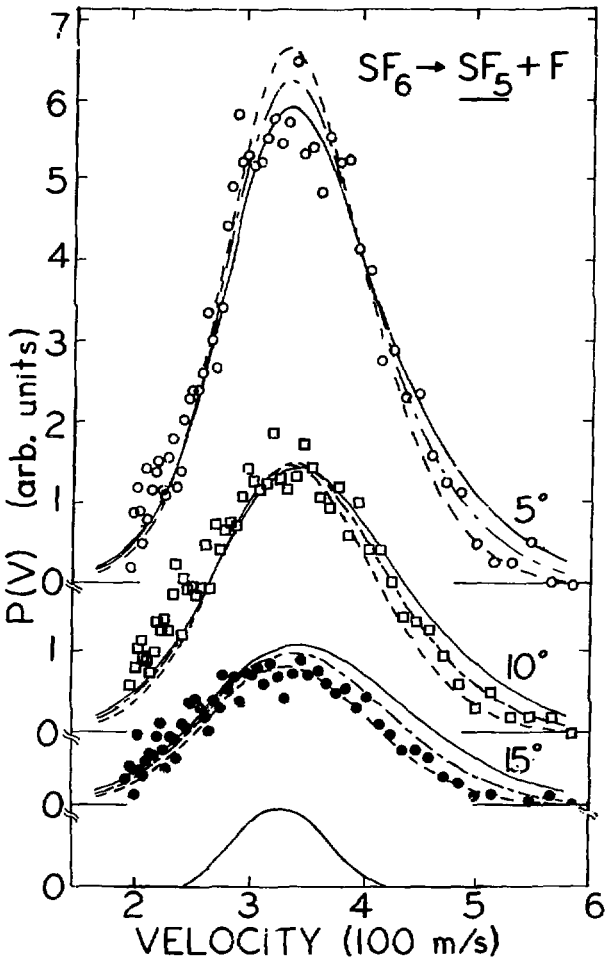

XBL 792-8359

Fig. 3

Fig. 4. Predicted translational energy distribution for the RRKM calculation of the SF_6 dissociation using 2, 3, 5, 8 and 12 excess photons.

—— – – —— 2 excess photons

• • • • • • • • 3 excess photons

— — — — 5 excess photons

—— – —— 8 excess photons

———————— 12 excess photons

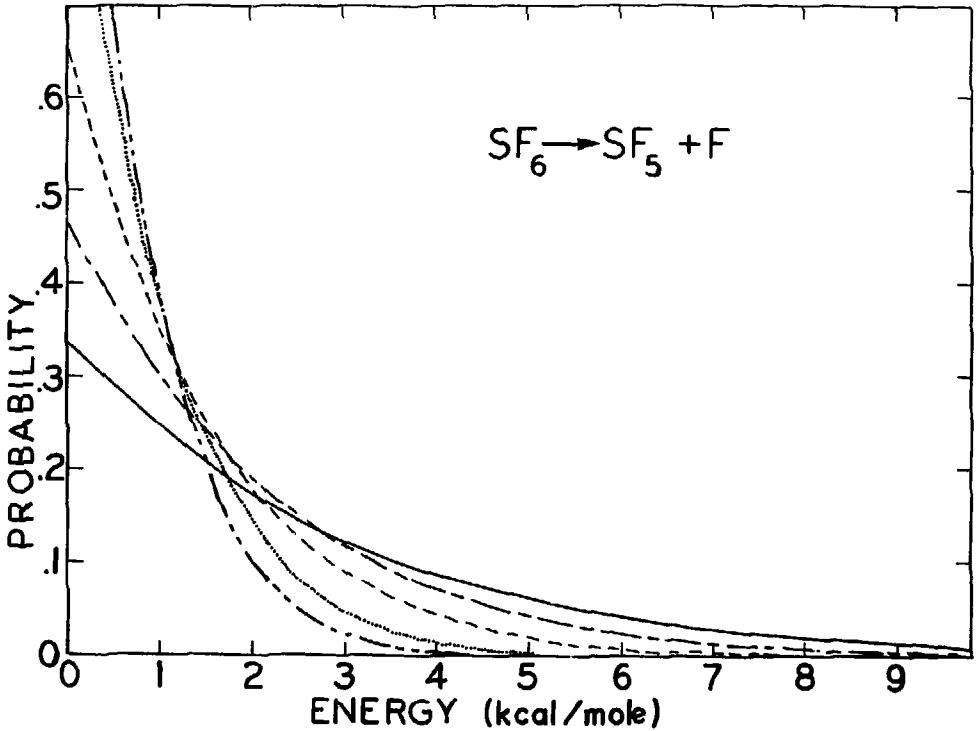

XBL 792-8354

Fig. 4

The results we obtain from the study of angular and velocity distribution of fragments are summarized as follows: 1) the translational energy distribution peaks at less than 0.2 kcal/mole. This means that no appreciable exit potential energy barrier exists along the reaction coordinate. It also implies no significant centrifugal barrier; thus, SF_6 must have acquired negligible average angular momentum in the multiphoton excitation process. 2) The fit of the RRKM translational energy distributions to the experimental ones indicates that at an energy fluence of $5J/cm^2$, the SF_6 molecules achieve excess energies of 16 to 27 kcal/mole before dissociating. 3) Of the 16 to 27 kcal/mole excess energy, only an average of 2.5 kcal/mole appears as translational energy of the fragments. 4) Because the rotational and translational energies are small, most of the excess energy is left as internal excitation in SF_5 (13 to 24 kcal/mole). Consequently the SF_5 fragment is already excited to the quasi-continuum. It can readily absorb more radiation, even if the laser frequency is significantly different from the fundamental absorption frequency of ground state SF_5. With sufficient energy fluence, SF_5 is excited beyond its own dissociation energy, and dissociates into $SF_4 + F$.

An attempt was made to find the translational energy of SF_4 and F produced in the secondary MPD of SF_5. The angular distribution is obtained over a limited range of angles ($>15^0$) where the $SF_3^+ : SF_2^+$ ratio is measured to be about 2.5:1 so that the MPD fragment is mainly SF_4. At angles less than 15^0 the $SF_3^+ : SF_2^+$ ratio is significantly larger than 2.5:1, even with a laser energy fluence of 50 J/cm^2. At these high energy fluences, the laser does not uniformly illuminate the interaction

region so that a considerable amount of SF_6, subject to energy fluences below 10 J/cm^2, does not undergo a two step dissociation to form SF_4. With the limited angular range over which the SF_4 fragment could be measured, the average translational energy released in the fragmentation $SF_5 \rightarrow SF_4+F$ could be determined only approximately. We find that the average energy released is between 0.5 and 1.5 kcal/mole.

Figure 5 shows the angular distribution of SF_3^+ obtained with 5 J/cm^2 and 3 J/cm^2 laser pulses and a 2.5 J/cm^2 pulse shortened by a plasma shutter. The RRKM theoretical calculations for the angular distributions at various excess energies are shown for comparison. The fits to the angular distributions obtained with 5 and 3 J/cm^2 pulses have average excess energies of ~22 kcal/mole (8 CO_2 laser photons) and ~13 kcal/mole (5 CO_2 laser photons), respectively. The 2.5 J/cm^2 shuttered pulse seems to have excess energy less than 8 kcal/mole (<3 CO_2 laser photons). The corresponding dissociation lifetimes predicted by the RRKM theory are 20 ns, 1 μs, and 20 μs, respectively. It should be noted that using the 2.5 J/cm^2 pulse, the angular distribution appears to deviate from the RRKM prediction. This is due to our experimental arrangement. In our apparatus (although the entire interaction region is monitored by the detector at all angles) the segment of the molecular beam monitored by the detector varies with the angular position of the detector. At 5 degrees, a 15 mm long segment is monitored, but at 25 degrees, only a 3 mm segment is monitored. The corresponding transit times for SF_6 to move through the detectable segment are 50 μs and 10 μs respectively. Therefore, any SF_6 molecules that absorb less than four excess photons have life times longer

Fig. 5. Angular distribution of SF_3^+ using:

△ 5 J/cm^2 , 60 ns pulse

● 3 J/cm^2 , 60 ns pulse

▲ 2.5 J/cm^2, 15 ns pulse.

The angular distributions are compared with the RRKM predicted angular distributions for 2, 3, 5, 8 and 12 excess photons. Symbols as in Fig. 4.

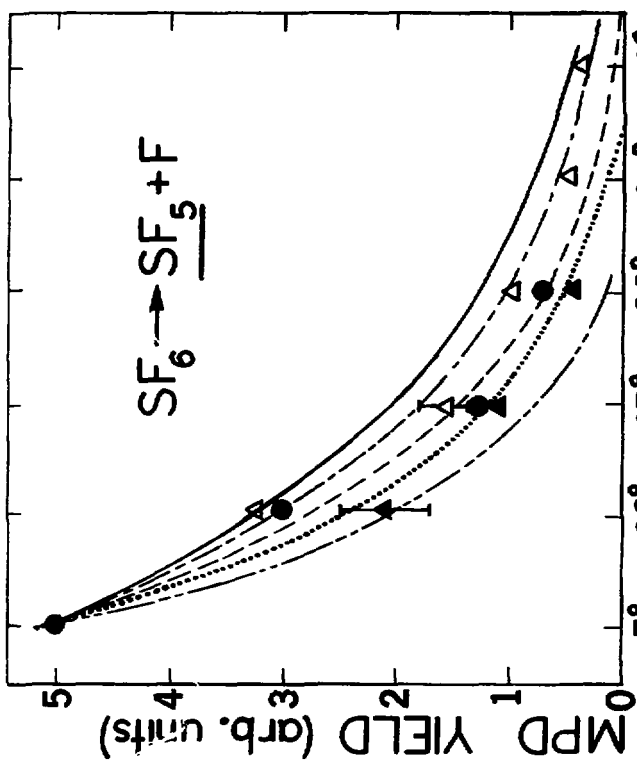

XBL 785-8834

Fig. 5

than 10 μs, than the transit time through the interaction region and can be seen by the detector only at small angles. Consequently, the observed angular distribution of SF_5 is weighted toward small angles and appears more sharply peaked than the RRKM prediction.

Figure 6 shows the frequency dependence of SF_6 MPD for vibrational temperatures between 210K and 450K. The energy fluence used is 5 J/cm^2 with a maximum power density over 100 MW/cm^2. The MPD yield spectrum is effectively broadened from 8.5 cm^{-1} at 210K to 18 cm^{-1} at 380K to >20 cm^{-1} at 450K. The MPD yield spectrum at 295K has a peak at ~943 cm^{-1} and a FWHM spread of ~14 cm^{-1}. This result qualitatively agrees with that reported by Ambartzumian et al.[3] whose spectrum has a peak at 941 cm^{-1} and a spread of ~18 cm^{-1}. When the vibrational temperature is either raised or lowered, the yield remains approximately the same at frequencies higher than 943 cm^{-1}. At lower frequencies, raising the vibrational temperature dramatically increases the MPD yield. These results suggest that the dissociation yield at higher laser frequencies (>943 cm^{-1}) is limited only by excitation through the quasi-continuum while the dissociation yield at lower frequencies is limited by excitation over the discrete levels. We show in Table 1 the vibrational population distributions at the four temperatures used in this experiment. At 210K 63% of the molecules are in the ground vibrational state. Therefore, the frequency dependence of MPD at 210K probably reflects quite closely the frequency dependence of MPD of ground vibrational state SF_6. The presence of vibrationally hot molecules at room temperature affects the MPD yield spectrum by increasing the amount of dissociation at low frequency. Cooling of SF_6 thus results in the disappearance of MPD at low frequency.

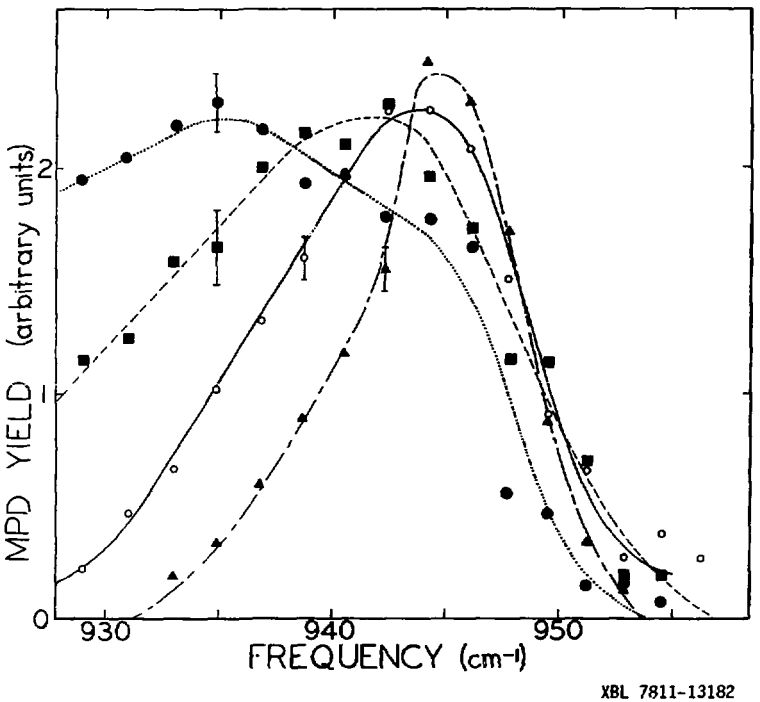

Fig. 6. Frequency dependence of SF_6 MPD at vibrational temperatures:

— — — 210K

——————— 300K

— — — 380K

..... 450 K

Table I. Population Distribution of SF_6 at Different Temperatures

	T_v	$E_{Ground\ State}$	P_o	$P_{\leq 1\ photon}$	$P_{\geq 2\ photon}$	$P_{\geq 3\ photon}$
(146 cm^{-1})	210 K	200 cm^{-1}	0.63	0.05	0.00	0.00
(208 cm^{-1})	300 K	600 cm^{-1}	0.30	0.27	0.016	0.001
(264 cm^{-1})	380 K	1080 cm^{-1}	0.15	0.46	0.09	0.014
(312 cm^{-1})	450 K	1570 cm^{-1}	0.07	0.68	0.24	0.06

Many gas cell experiments have been performed to measure the SF_6 MPD yield as a function of energy fluence at several different CO_2 laser frequencies. Kwok and Yablonovitch[22] have recently shown that even for SF_6 barely excited to the quasi-continuum, the collisional relaxation time is τ_{coll} = 13 ns-torr/p where p is the SF_6 gas pressure. In a gas cell experiment holes burned in the rotational population distribution by the laser may be filled by collisional relaxation even at moderately low pressures. Then, both the energy fluence and frequency dependences of the MPD yield are affected. Therefore it is important to measure these dependences in a collision-free molecular beam experiment.

Figure 7 shows the energy fluence dependence of MPD of SF_6 at three different laser frequencies. Since the experiments are performed with the same laser pulse duration, it is important to note that the power of the laser is also varied proportional to energy fluence. At 935 cm^{-1}, MPD is observed at energy fluences as low as 1-2 J/cm^2 and the yield increases slowly with increasing energy fluence. At 944 cm^{-1} the SF_6 MPD threshold is observed at higher energy fluence but the dissociation yield increases very rapidly with increasing fluence. At 953 cm^{-1} SF_6 MPD is first observed at even higher fluence, but the yield increases slowly with fluence. Measurements at other frequencies between 935 and 953 cm^{-1} have also been made; the yield curves are intermediate between the ones shown. Figure 8 shows the energy fluence threshold for dissociation as a function of frequency obtained from plots similar to Figure 7. Our results agree with those of Gower and Billman[23] and disagree with those of Brunner and Proch[24], that is, the threshold at 935 cm^{-1} is four times lower than the

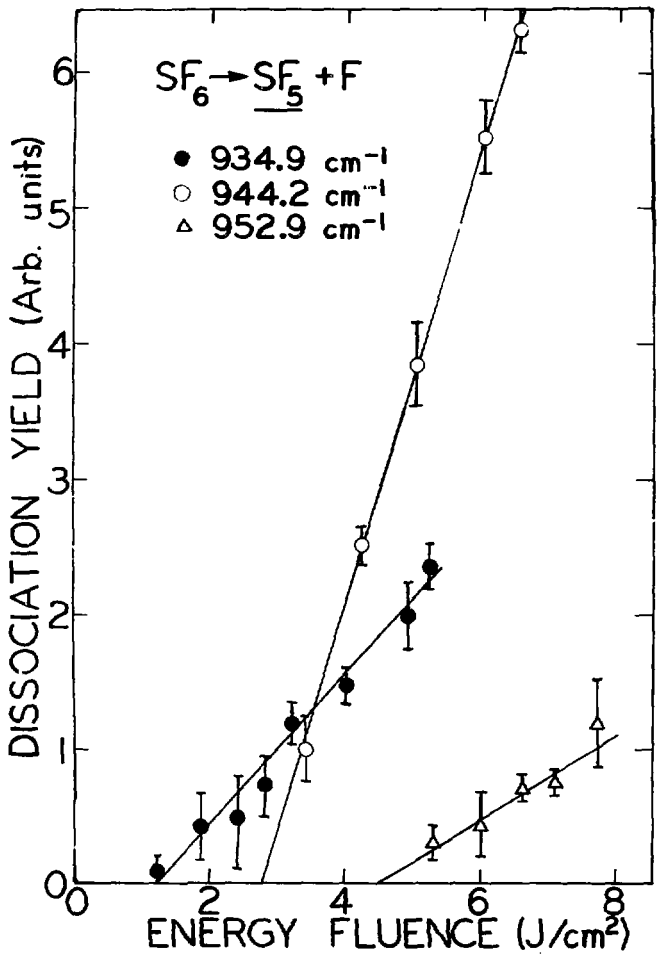

XBL 792-8358

Fig. 7. Energy fluence dependence of SF_6 MPD at three CO_2 laser frequencies.

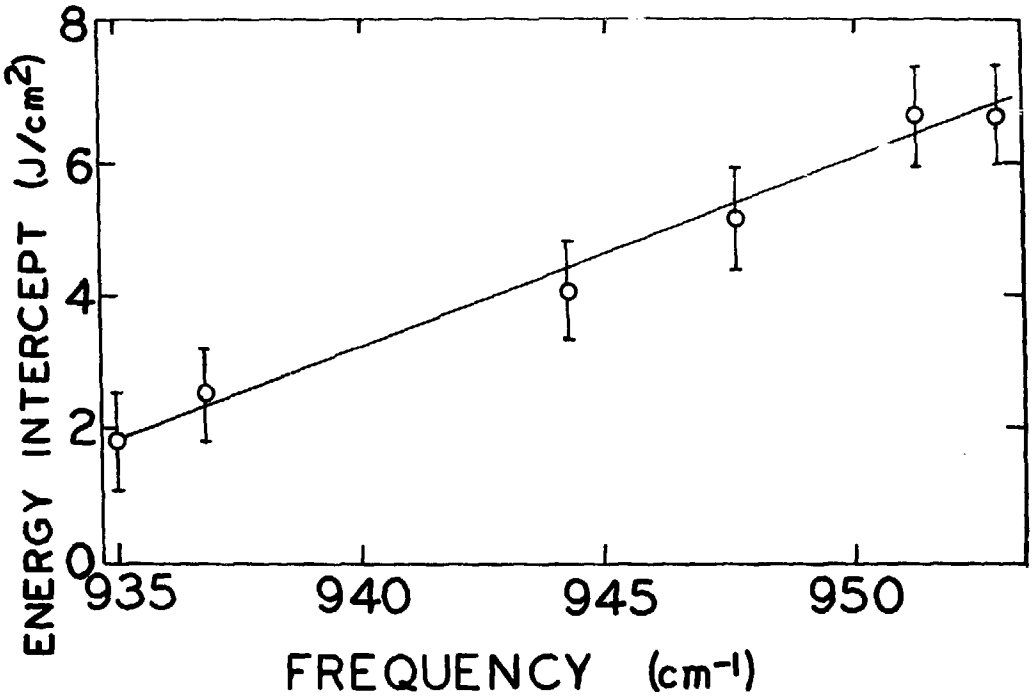

Fig. 8. Minimum energy fluence at which detectable SF_3^+ signal could be observed as a function of frequency.

XBL 792-8282

threshold at 952 cm^{-1}. The low energy fluence threshold at low frequency is caused by a larger quasi-continuum cross section at low frequency. However, the bottleneck prevents a lot of dissociation from occurring at low frequency. At high frequency (near the ν_3 resonance) the quasi-continuum cross section is small so the energy fluence threshold is large and the bottleneck is relatively unimportant.

In general the experimental results are affected by several important factors. We briefly describe these factors here and again in more detail in the discussion section.

(1) The hot band absorption becomes increasingly important at higher temperatures and at frequencies below 943 cm^{-1}. It lowers the laser intensity necessary to pump the molecules into the quasi-continuum.

(2) Low intensity laser radiation is only effective in exciting a small fraction of the rotational population into the quasi-continuum. Thus, the frequency dependence of MPD at low laser intensity should depend on the population distribution in the rotational states.

(3) With the laser pulse duration kept constant, increasing the energy fluence increases the intensity. The increased intensity results in more molecules pumped into the quasi-continuum.

(4) The absorption spectrum of molecules in the quasi-continuum shifts to lower frequency as the level of excitation increases. This has been shown by the experiments of Nowak and Lyman[25] and Bott.[26]

Two frequency experiments are designed to decouple the absorption in the region of the discrete vibrational ladder from that in the quasi-continuum. The first laser excites a certain fraction of the SF_6 molecules into the quasi-continuum where some further excitation

may occur, depending on the energy fluence in the pulse.[27] The second laser then interacts with three different groups of SF_6 molecules: (1) ground state molecules, (2) vibrationally excited molecules in the low lying discrete levels, and (3) molecules in the quasi-continuum. By being sure that the second laser alone does not cause dissociation of SF_6, we can neglect the contribution of the ground state SF_6 to the dissociation yield. If the second laser is at a frequency sufficiently far above the molecular resonant frequency, the MPD of vibrationally excited molecules in the discrete levels also becomes relatively insignificant.

Figure 9 gives our results on the frequency dependence of the MPD yield of SF_6 using two lasers, one fixed at 1060 cm^{-1} and the other tuned through the ν_3 resonance of SF_6. It is seen that the dependence of MPD on the frequency of the second laser is significantly narrower and shifted to higher frequency than the one obtained with a single laser. These results are in good agreement with those of Ambartzumian et al.[28] The major reason for the change in the frequency dependence is that the intensity of the tuned laser in the two laser experiment is lower than that in the one laser experiment. The decreased intensity reduces the range of initial states that are coupled to the quasi-continuum by the laser and results in a smaller MPD frequency spread.

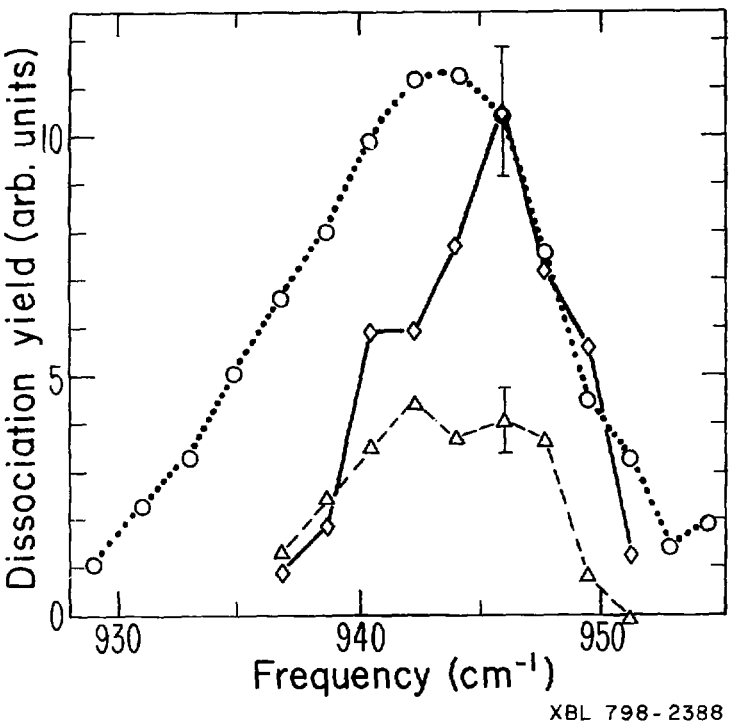

Fig. 9. Frequency spectrum of SF_6 absorption with a weak CO_2 laser pulse. Detection was achieved by dissociation with a 10 J/cm^2 laser pulse at 1060 cm^{-1}.

○ ····· 5 J/cm^2 pulse - single frequency only

◇ ———— 1.2 J/cm^2 pulse

△ — — — 0.5 J/cm^2 pulse

The relative size of the signal for the 1.2 and 0.5 J/cm^2 pulses is shown in the figure. Otherwise the scale is arbitrary.

MODEL CALCULATIONS

Recently, a number of calculations have been performed on the infrared MPD of SF_6[15,16,29] using the rate equation model. Here we extend the model calculations by explicitly considering the intensity dependent excitation over the discrete levels into the quasi-continuum and the two step dissociation process: $SF_6 \rightarrow SF_5 + F \rightarrow SF_4 + 2F$. These model calculations are compared with the experimental results just described. The good agreement between the model and the experiments implies that the model calculation provides a quantitative description of MPD of SF_6.

The rate equation model proposed in reference 15 is based on the following assumptions:

(1) The MPD yield is determined by the multiple stepwise excitation in the quasi-continuum and is not limited by the excitation over discrete levels.

(2) Coherent optical effects, spontaneous emission, and collisions are neglected in the excitation process.

(3) All molecules at approximately the same energy have the same absorption cross section.

(4) The ratio of the stimulated emission cross section to the absorption cross section is given by the ratio of the density of states of SF_6 in the levels involved.

(5) The dissociation rate constant at a given energy above the dissociation energy is given by the statistical RRKM model.

(6) The SF_5 dissociation product absorbs an insignificant amount of energy from the infrared field and thus any secondary MPD is ignored.

Here we present the model calculation with assumptions 1 and 6 eliminated. Following assumptions (2)-(5) the rate equations for molecules in the quasi-continuum are:

$$\frac{dN_m}{dt} = \frac{I(t)}{h\nu}\left[\sigma_{m-1}N_{m-1} + \frac{g_m}{g_{m+1}}\sigma_m N_{m+1} - \left(\frac{g_{m-1}}{g_m}\sigma_{m-1}+\sigma_m\right)N_m\right] - k_m N_m \quad (1)$$

where N_m is the normalized population in level m at energy $mh\nu$, $I(t)$ is the laser intensity, g_m is the density of states of level m, σ_m is the absorption cross section from level m to level m + 1, and k_m is the dissociation rate constant from level m calculated using the RRKM model (see appendix). The use of the RRKM model was justified in the previous section.

It is easily seen from Eq. (1) that if the dissociation is insignificant ($k_m = 0$), the excitation rate is proportional to the laser intensity. Time integration of the rate equations gives a population distribution which is only a function of laser energy fluence. In fact, our calculations show that for a given laser energy fluence the dissociation does not strongly affect the shape of the population distribution below the dissociation levels even if a significant fraction of the SF_6 has dissociated. This makes energy fluence an important parameter in the model calculation.

The density of states, g_m, is calculated with the Whitten-Rabinovitch approximation.[20] Use of this approximation tacitly assumes that the SF_6 molecules in the quasi-continuum are randomly distributed in the available vibrational states. There is the question of whether the rotational degrees of freedom should be included in the calculation of the density of states. The upper limit of this effect is investigated

by calculating the density of states with the rovibrational Whitten-Rabinovitch approximation.[20] At the onset of the quasi-continuum the ratio of density of states changes by only 4% (i.e., $(g_4/g_3)_{v,r} = 1.04(g_4/g_3)_v$), while at the dissociation level it changes by only 1%. These changes cause at most a 1% difference in the population of any level in a typical model calculation. Thus, inclusion of rotational degrees of freedom in the calculation of the density of states is not important in this rate equation model.

The absorption cross section and its dependence on excitation energy are very difficult to estimate from any ab-initio calculation. In our calculation the absorption cross section is assumed to decrease exponentially with excitation and is determined by a fit to the expermental results as we shall describe later.

To include multiphoton excitation of the SF_5 dissociation product and the subsequent secondary dissociation into SF_4+F in the model calculation, there should be a similar set of rate equations for SF_5:

$$\frac{dN_j(SF_5)}{dt} = \frac{I(t)}{h\nu}\left[\sigma_{j-1}N_{j-1}(SF_5) + \frac{g_j\sigma_j}{g_{j+1}}N_{j+1}(SF_5) - \left(\frac{g_{j-1}}{g_j}\sigma_{j-1} + \sigma_j\right)N_j(SF_5)\right] - k_jN_j(SF_5) + k_mN_m(SF_6) \qquad (2)$$

where $m = j + D/h\nu$ and D is the dissociation energy of SF_6. The term involving $N_m(SF_6)$, indicates generation of SF_5 through dissociation of SF_6. Because the translational energy of the fragments is only a small fraction of the excess energy beyond the dissociation energy,

we assume that all the excess energy in SF_6 appears as internal energy in SF_5. Thus, the rate of appearance of SF_5 in a given level equals the dissociation rate of SF_6 from the corresponding level. The density of states for SF_5 is obtained from the Whitten-Rabinovitch approximation and the SF_5 dissociation rate constants from an RRKM calculation (see appendix). The absorption cross section is found by a fit of the calculation to the experimental data on the MPD of SF_5. The inclusion of multiphoton excitation of the SF_5 dissociation product provides a more accurate description of MPD of SF_6.

A more realistic model calculation should also include the intensity dependent 3-6 photon excitation over the discrete levels of SF_6. The existence of an intensity dependent "bottleneck" in the excitation into the quasi-continuum was originally suggested by Ambartzumian et al.[3] and subsequently shown experimentally.[14,28] Detailed quantum mechanical models of the discrete levels have been developed [3,30] which include the rotational substructure in the vibrational levels. The time development of the excited SF_6 population in the discrete levels has been calculated using such models.[31,32] However, they are too complex for simple calculation. We use here a much simpler, phenomenological approach.

The major assumption in this approach is that the excitation of population into the quasi-continuum from different rotational vibrational states requires different laser intensities. The bottleneck is a consequence of the fact that not all the molecules are in a single rotational-vibrational state. To illustrate this, assume that the quasi-continuum begins at an energy of $3h\nu$ and that a single three

photon process is effective in exciting the population into the quasi-continuum. If we neglect stimulated emission, then the excitation rate can be assumed to be proportional to I^3. The rate of depletion of population, $N_{0,J}$, in the Jth rotational level of the ground vibrational state is given by:

$$\frac{dN_{0,J}}{dt} = -a_J I^3 N_{0,J}$$

and the solution is:

$$N_{0,J} = N_{0,J}(0) \exp\left[-a_J \int_0^t I^3(t')dt'\right] \tag{3}$$

where a_J is a constant different for different rotational-vibrational states. The rate at which the population is excited into the quasi-continuum is then equal to $-d(\sum_J N_{0,J}(t))/dt$. This should be included in the rate equation for m = 3 in Eq. 1 as an additional source term, i.e.,

$$\frac{dN_3}{dt} = \frac{g_3}{g_4}\sigma_3 N_4 - \sigma_3 N_3 - \frac{d}{dt}\left(\sum_J N_{0,J}\right) \tag{4}$$

For a usual bell-shaped pulse, the function $N_{0,J}(t)$ is close to a step function and can be further approximated by:

$$N_{0,J}(t) = N_{0,J}(0) \quad \text{if } I_{max}(t) \leq I_J$$
$$= 0 \quad \text{if } I_{max}(t) > I_J$$

where $I_{max}(t)$ is the maximum laser intensity during the time period between $-\infty$ and t and I_J is a value characteristic of the excitation of the Jth rotational-vibrational state to the quasi-continuum. This

is a reasonable approximation; it also makes the model insensitive to the exact excitation mechanism over the discrete levels which is probably not a single three photon process.[30-32] It should also be noted that $N_{0,J}$ only depends on $I_{max}(t)$.

For each of the many rotational states there is a different intensity, I_J, required to excite the molecules over the discrete states into the quasi-continuum. The I_J's are spread over a wide range of intensities reflecting the fact that the detuning of the laser frequency from resonance may be dramatically different for different rotational states. We therefore assume that the I_J's are approximated by a continuous distribution. The resulting $\sum N_{0,J}(I_{max}(t))$, instead of being a sum of step functions, becomes a continuously differentiable function. This function should satisfy the condition that very little population is excited over the discrete states into the quasi-continuum when the peak laser intensity, $I_{max}(t)$, is small. If the peak laser intensity is large nearly all the population should be excited over the discrete states into the quasi-continuum. As shown in Fig. 10 the curve represented by the function:

$$\sum_J N_{0,J}(I_{max}(t)) = \frac{1}{\sqrt{\pi}} \int_{\gamma \ln(I_{max}(t)/I_o)}^{\infty} e^{-x^2} dx$$

has these properties, e.g., $\sum_J N_{0,J} \to 1$ when I_{max} is small and $\sum_J N_{0,J} \to 0$ when I_{max} is large. Here, I_o is the median of the I_J's and γ is a parameter characterizing the spread of I_J's.

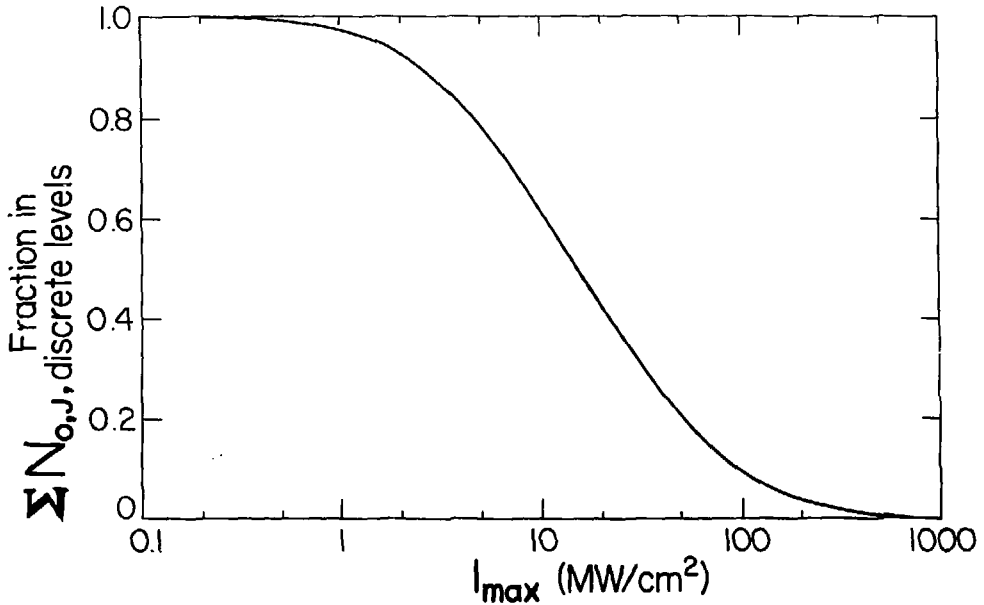

Fig. 10. Model used for excitation over the discrete states. The fraction of molecules excited to the quasi-continuum is assumed to be a function of intensity only. See text for functional form.

XBL 795-1654A

This model is used to calculate the MPD of SF_6. The algorithm is a simple time integration of Eq. 1, 2, 4, and 6 with the initial condition that all the population is initially in the lowest level. By varying the time step for integration around 10ps, it is ascertained that round off errors are negligible. The laser pulse profile, I(t), used in these calculations is shown in Fig. 11 and is representative of the pulse envelope from a Tachisto 215G laser ignoring the mode locking spikes of the pulse. The mode locking spikes in the 60ns multimode pulse were considered in our calculation by assuming that the mode locking doubles the peak intensity achieved by a single mode pulse. The limited time resolution of the detector and oscilloscope prevented us from measuring the actual peak intensity.

With the quasi-continuum absorption cross section assumed to have the form $\sigma_m = \sigma_0 e^{-\beta m}$, there are four independent parameters to be determined: γ and I_0 for excitation up the discrete vibrational ladder and σ_0 and β for excitation through the quasi-continuum. The parameters are chosen to fit the experimental results of Black et al.[12] on the average number of photons absorbed per molecule, <n>, versus energy fluence at 944 cm^{-1} using three different laser pulses: 0.6ns and 60ns single mode and 60ns multimode. We find that our calculation closely reproduces the experimental curves of Black et al.[12] with $\gamma = .5$, $I_0 = 20$ MW/cm^2, $\sigma_0 = 8\times10^{-19}$ cm^2, and $\beta = .042$. This is shown in Fig. 12. The fit to the 0.6 ns pulse is insensitive to the parameters γ and I_0 in the calculation because the maximum laser intensity is much larger than I_0. So, the 0.6 ns pulse result is used to find σ_0 and β and the 60ns single mode pulse result is used to find γ and I_0.

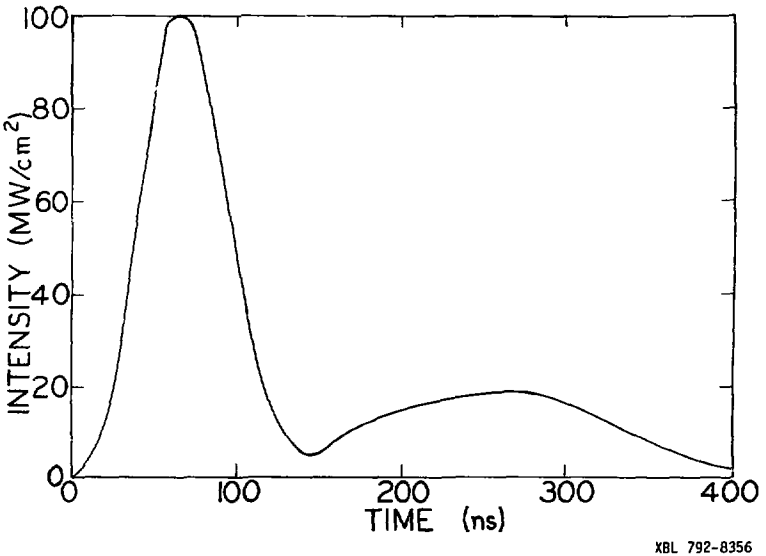

Fig. 11. Typical laser pulse shape used in the model calculation in the text. The energy fluence is 10 J/cm^2, 40% of which is in the tail.

Fig. 12. Energy deposition in SF_6. <n> versus energy fluence predicted by the model calculation for two different pulse lengths 60 ns and 0.6 ns. These are compared with the experimental data of Black, et al.

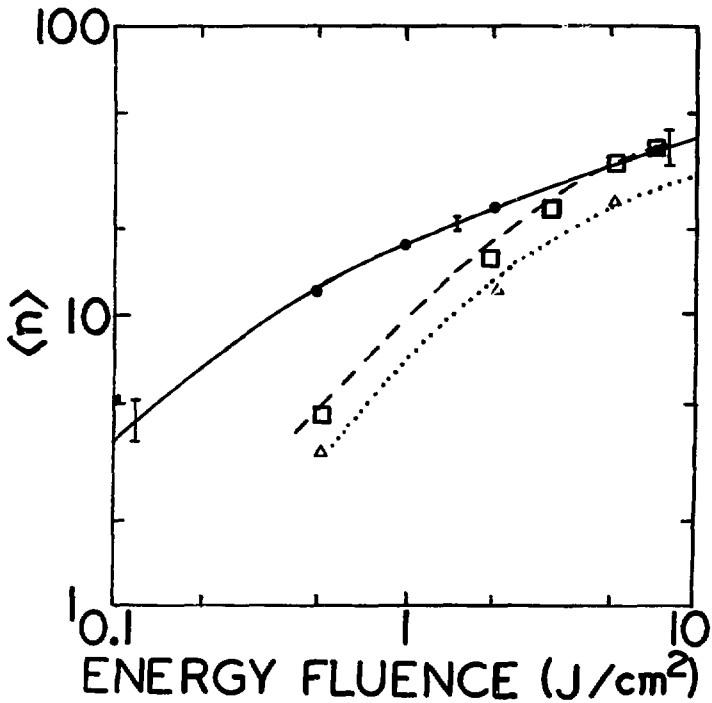

XBL 792-8281

Fig. 12

The 60ns multimode pulse result agrees qualitatively with the model calculation, but seems to indicate that the intensity is more than twice the intensity of the single mode pulse, which is the assumption in the model calculation. That the multimode pulse achieves more than double the intensity of a single mode pulse has been observed by other groups using faster detectors and oscilloscopes.

The results obtained in our molecular beam apparatus are the only data on the multiphoton dissociation of SF_5. Therefore, we assume, from lack of data to the contrary, that the discrete vibrational states of SF_5 can be neglected because the SF_5 has enough vibrational energy to be in its quasi-continuum and that its quasi-continuum cross section is independent of the SF_5 energy (i.e., $\beta = 0$). The onset of secondary MPD of SF_5 observed experimentally agrees with the results of the model calculation using $\sigma_o = 10^{-19}$ cm^2.

Figure 13 shows our model calculation for the dissociation yield versus energy fluence using a 60ns multimode laser pulse. The yield is nearly linear in energy fluence from 3 to 7 J/cm^2 in excellent agreement with the linear dependence experimentally observed at 944 cm^{-1} (see Fig. 7). At higher fluence, the SF_5 product disappears because it dissociates into SF_4 + F. The SF_4 yield grows quickly with energy fluence until there is 100% yield.

Grant et al.[15] showed that the population distribution in the quasi-continuum predicted by a model with no bottleneck is significantly narrower than a thermal distribution. The conclusion is also valid for this model calculation when the intensity dependence of excitation over the discrete levels is included. The model calculation with a

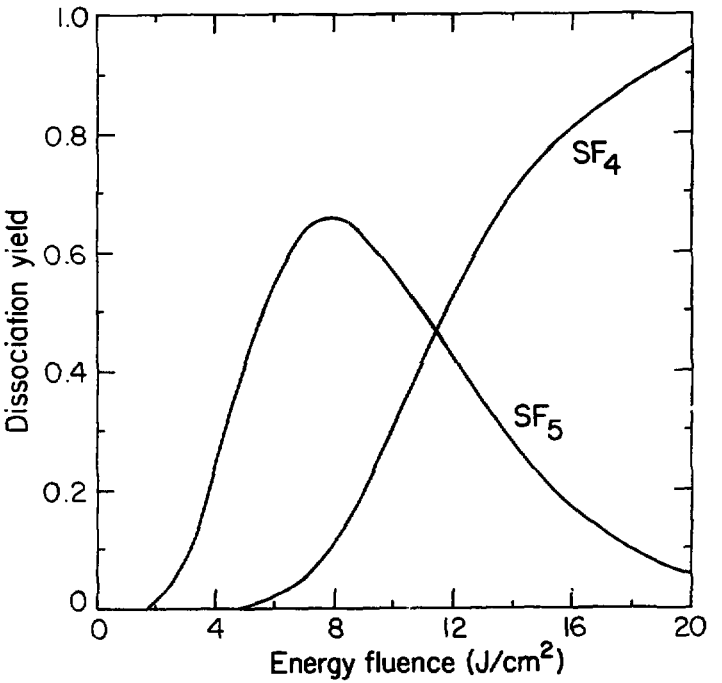

XBL 795-1653

Fig. 13. SF_6 yield into SF_5 and SF_4 as a function of energy fluence predicted by the model calculation. Only those molecules which can be detected in our molecular beam experiment (lifetime less than 10 μs) are considered.

0.5 J/cm^2, 60ns FWHM laser pulse predicts that the population in the quasi-continuum is narrower than thermal even though only 20% of the molecules have been excited over the discrete states into the quasi-continuum. The population distribution is narrower than thermal whenever the cross section decreases with increasing excitation because the excitation rate for those molecules in the low energy tail of the distribution is large and the excitation rate in the high energy tail is small. Fig. 14 shows a comparison of the population distribution for a .5J/cm^2, 60ns laser pulse and for a .5J/cm^2, 15ns FWHM plasma shuttered laser pulse from our model calculations. In both cases the predicted population distribution is narrower than thermal. Because the plasma shuttered pulse achieves a higher intensity, the model predicts that more population is coupled into the quasi-continuum. The shape of the population distributions shown in Fig. 14 are similar but differ slightly because the maximum intensity of the shuttered pulse occurs at the end of the pulse, so population is being excited into the quasi-continuum at the end of the pulse. Thus, the shuttered pulse is slightly broader and peaks at a slightly lower energy. As the energy fluence is increased above .5 J/cm^2 the slight effect of the laser pulse shape on the population distribution becomes undetectable. The shape of the SF_6 population distribution is almost completely determined by the energy fluence if the energy fluence is greater than .5J/cm^2 and the laser pulse duration is less than 100ns. Because the quasi-continuum cross section decreases with increasing energy at 944 cm^{-1}, the population distribution is also narrower than a thermal distribution even if a bottleneck is included in the model calculation.

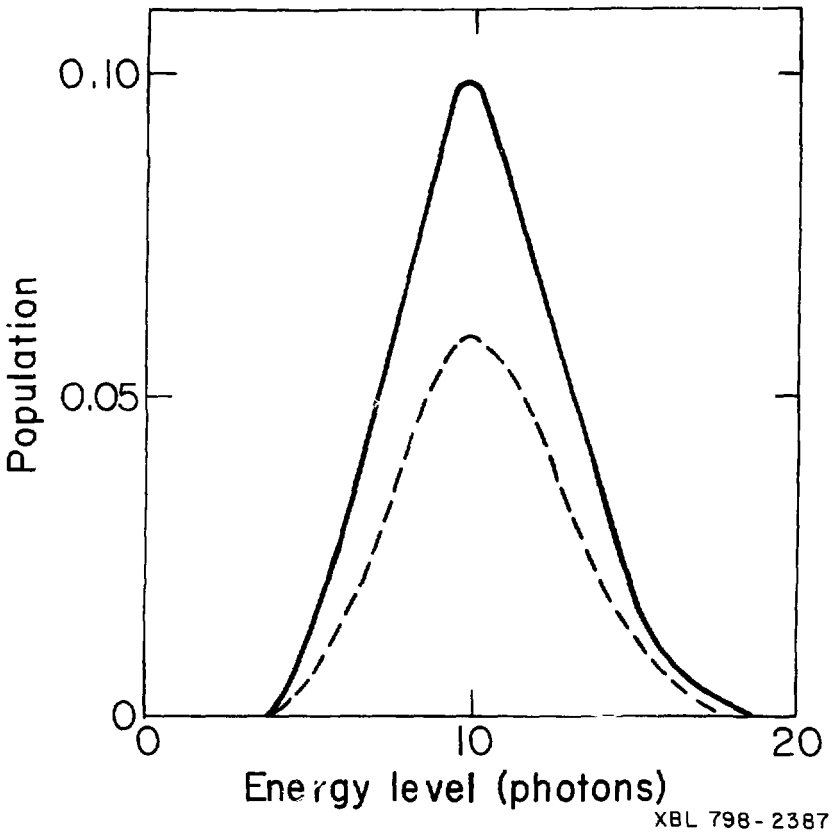

Fig. 14. Calculation of multiphoton excited SF_6 distribution predicted by model calculation using $0.3^6 J/cm^2$ laser pulse.

——————— 15 ns FWHM - shuttered pulse

— — — — 60 ns FWHM pulse

Our calculation also answers the question of how the laser intensity affects the distribution of excess energies with which SF_6 dissociates. At energy fluences greater than about 10 J/cm^2 the average level from which dissociation occurs is determined by the intensity for pulse durations longer than 0.6 ns. We call this regime lifetime limited because dissocation occurs primarily from levels where the RRKM predicted dissociation rate is approximately equal to the up-excitation rate. At energy fluences below about 5 J/cm^2 the calculation predicts that most of the dissociation occurs after the laser pulse is over. Then, it is the energy fluence and not the intensity which determines the average dissociation level. Figure 15 illustrates both of these considerations by showing the distribution of excess energies from which SF_6 dissociates into SF_5 + F using a 7.5 J/cm^2 laser pulse at two different pulse durations - 60ns and 0.6ns FWHM. Because the up-excitation rate is much faster with a short, high intensity laser pulse, the average excess energy is higher. However, a considerable fraction of the molecules do not dissociate during the laser pulse and are subject only to the limitation of energy fluence so that there is a long tail of population which dissociates with low excess energy. Thus, as the laser pulse duration is decreased at constant energy fluence, the molecules at first dissociate from higher energy corresponding to shorter lifetimes. In this lifetime limited region, up-excitation is balanced by dissociation. However, as the pulse duration is decreased further and in the limit of zero pulse duration, the molecules can be pumped to energy levels no higher than the levels allowed by energy fluence considerations.

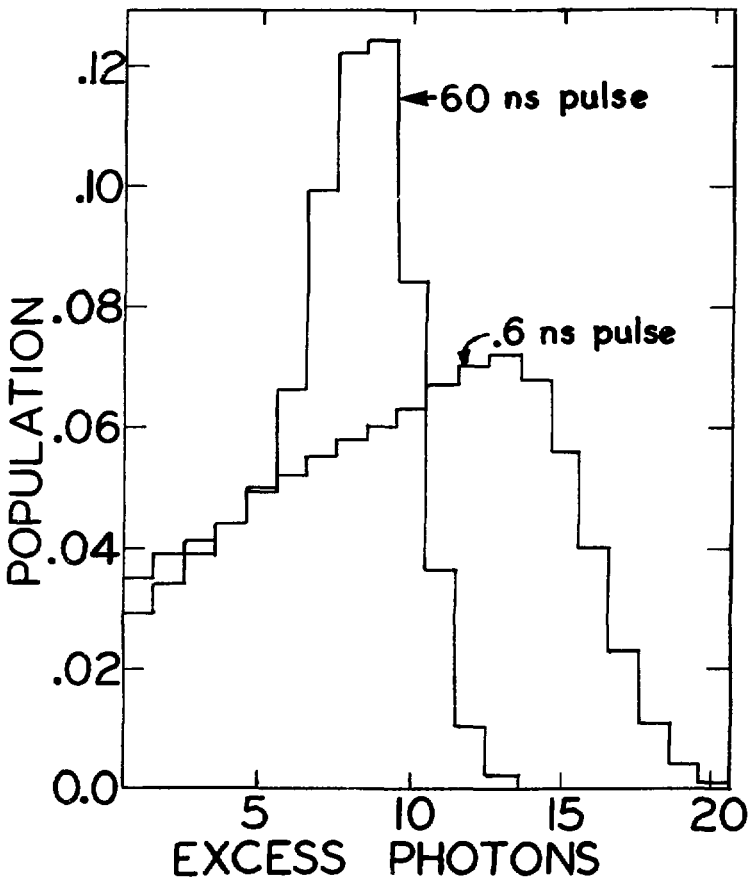

XBL 798-11021

Fig. 15. Model calculation of the distribution of excess energies with which SF_6 dissociates for a 7.5 J/cm^2 pulse at pulse durations of 60 ns and 0.6 ns.

Figure 16 shows the SF_5 population distribution from the model calculation for a 7.5 J/cm^2 laser pulse for the same two pulse durations - 60ns and 0.6ns FWHM. The figure shows that the average energy in SF_5 is nearly independent of the laser pulse duration. This is caused by the SF_5 quasi-continuum cross section and the SF_6 cross section above the dissociation energy being roughly the same in our model calculation. As discussed earlier, these cross sections, determined from theoretical fits of the experimental results, are about 1-2 x 10^{-19} cm^2 for SF_6 above the dissociation energy and 10^{-19} cm^2 for SF_5 in the quasi-continuum. Thus the net rate of excitation for SF_5 in the quasi-continuum and SF_6 excited above its dissociation energy are nearly the same. Most of the excess energy pumped into SF_6 appears as internal energy of SF_5. Therefore, the average energy in SF_5 does not depend very much on the amount of excess energy SF_6 has when it dissociates. Hence, it does not depend on the laser pulse duration. The shape of the SF_5 distribution is determined by (1) the distribution of excess energies with which SF_6 dissociates after the laser pulse and (2) the continuous up-pumping of population in the SF_5 quasi-continuum during the laser pulse. The SF_5 population distribution at 7.5 J/cm^2 is much broader than a thermal SF_5 distribution and is dominated by the SF_6 dissociation process. Our calculation predicts that 8% of the population is still in the discrete vibrational ladder for a 7.5 J/cm^2, 60ns laser pulse, which explains the somewhat smaller SF_5 population for the 60ns pulse than the 0.6ns pulse.

The model can also predict the dynamics of the SF_5 dissociation to SF_4 + F. For the 60 ns, 7.5 J/cm^2 pulse, the SF_5 molecules dissociate

Fig. 16. SF_5 population distributions immediately after irradiation of SF_6 with 7.5 J/cm^2 pulse of different durations. The dissociation energy of 51 kcal/mole is marked by the arrow.

———————— 0.6 ns FWHM pulse

—— —— 60 ns FWHM pulse

The dotted curves indicate the distributions long after the end of each laser pulse. After the end of the laser pulse, all SF_6 excited beyond the dissociation limit dissociates to SF_5, thus accounting for the increase in population of SF_5 shown by the dotted curves.

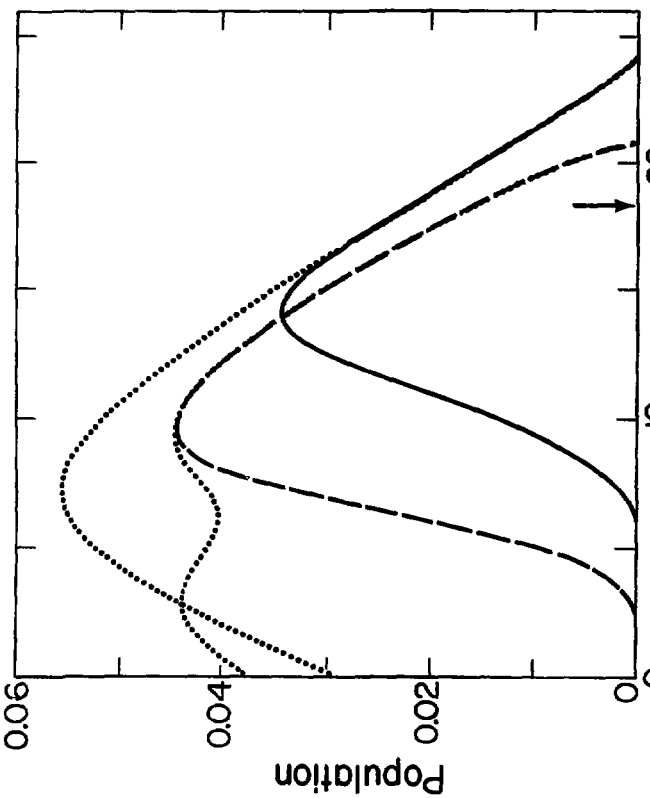

Fig. 16

XBL798-2390

with an average excess energy of ~6 kcal/mole. The RRKM calculation predicts that approximately 1 kcal/mole is released into translational energy. When the energy fluence is increased to 15 J/cm^2 the SF_5 dissociation is then in the lifetime limited regime, the average excess energy is ~9 kcal/mole, and an average of 1.5 kcal/mole is released into translation. These results are consistent with our experimental results and confirm the validity of our model for the two step dissociation process.

DISCUSSION

Our observations on the multiphoton dissociation of SF_6, like other simple bond rupture reactions studied by this group,[19] are consistent with the RRKM statistical theory as the description of unimolecular reactions in MPD. Specifically, (1) SF_6 dissociates through the lowest energy channel, $SF_5 + F$, (2) the observed SF_5 angular and velocity distributions can be fit with distributions calculated using RRKM theory, (3) the observed limits to the lifetime are in agreement with the RRKM predicted lifetime based on the excess energy which is used to fit the angular and velocity distributions, and (4) these results are in agreement with the predictions of the model calculations.

We expect that the amount of $SF_4 + F_2$ formed by SF_6 MPD is very small. However, the limited experimental sensitivity does not allow us to detect $SF_4 + F_2$ if those dissociation products are less than 20% of the SF_6 that dissociates via the $SF_5 + F$ channel. The RRKM calculation predicts the SF_6 dissociating to $SF_4 + F_2$ is several orders of magnitude smaller than the dissociation to $SF_5 + F$ for SF_6 internal energies up to 30 kcal/mole above the $SF_5 + F$ dissociation limit. The RRKM theory is thus consistent with our experimental observation of SF_5 being the major dissociation product.

The comparison between calculated and observed velocity and angular distributions was made in Figs. 3 and 5. The distributions for the 5 J/cm^2 pulse fit the RRKM predicted distributions using 8 excess photons. For a 3 J/cm^2 pulse a fit is achieved using 5 excess photons. Although the error bars are relatively large, the general shape of the RRKM distribution is confirmed. For the 2.5 J/cm^2 shuttered pulse,

the angular distribution differs somewhat from the RRKM prediction using 3 excess photons, because the RRKM lifetime is longer than the 10μs required to traverse the interaction region. This causes the angular distribution to peak at smaller angles as was discussed in the results and analysis section. After accounting for the finitie dissociation lifetime, this result also supports the validity of the RRKM theory.

If the dissociation lifetime is appreciably shorter than the laser pulse duration, secondary multiphoton dissociation of SF_5 to SF_4+F can occur. In our experiment with laser pulses of 60ns FWHM secondary dissociation started to appear at energy fluences of 10 J/cm^2. Thus, just below the onset of secondary dissociation the average dissociation lifetime of SF_6 should be close to 60ns. At 5 J/cm^2, somewhat below the onset of secondary dissociation, the dissociation lifetime is 50ns (8 excess photons). This result again supports the validity of the RRKM theory.

The validity of the RRKM theory indicates that even if energy is localized in certain modes immediately after the excitation, it is certainly randomized among essentially all the vibrational modes on a timescale much shorter than the dissociation lifetime. In SF_6 MPD at an intensity of 100 MW/cm^2, the net up-excitation rate is less than 10^8 photons absorbed/sec for excitation levels above the dissociation limit. Dissociation lifetimes are therefore no faster than $\sim 10^{-8}$ sec. The conclusion that energy is randomized in less than 10^{-8} sec is not surprising because many experiments, reviewed by Oref and Rabinovitch[33], show that intramolecular energy transfer rates

are greater than 10^{11} sec^{-1} for polyatomic molecules when excited beyond a dissociation energy of more than 40 kcal/mole.

Initial vibrational excitation of SF_6 prior to multiphoton excitation tends to diminish the bottleneck effect of the low-lying discrete levels and thus increases the MPD yield. In our experiments SF_6 was first excited either by thermal excitation or by laser excitation. The MPD yield was then measured after further laser excitation with enough fluence. From these experiments, we can conclude:

(1) Excitation over the discrete states has a spectrum fairly close to the linear absorption spectrum of the molecules if the laser intensity is not excessively high and molecules are not internally excited. Both the 210 K (see Fig. 6) and the two frequency (see Fig. 9) multiphoton dissociation have a frequency dependence that peaks 3-4 cm^{-1} below resonance and has a FWHM spread of ~8 cm^{-1}.

(2) The absorption spectrum shifts to lower frequency as the internal excitation increases. This is shown in the 450 K MPD yield frequency dependence which peaks ~15 cm^{-1} below the resonance.

Assuming that the pump pulse is intense enough to excite a large fraction of molecules into the quasi-continuum we could then determine crudely the dispersion of the average absorption cross section of molecules in the quasi-continuum of MPD by observing the change in energy fluence threshold with frequency (Fig. 8). This is because the average excitation in the quasi-continuum depends only upon the product of the cross section and the energy fluence so that the energy fluence required to observe MPD mear threshold should be inversely proportional to the average absorption cross section in the quasi-continuum. From

Fig. 8 and the results of Gower and Billman,[23] we may conclude that the cross section decreases by a factor of 4 ± 2 when the laser frequency changes 935 to 953 cm^{-1}. This result is in good agreement with the absorption cross section obtained by Nowak and Lyman[25] at high SF_6 temperatures.

Both the laser intensity and energy fluence are important in determining the MPD yield. As is now well known, excitation over the discrete levels into the quasi-continuum depends on the laser intensity. If the laser intensity is sufficiently strong, then most of the population is excited into the quasi-continuum. This is particularly true when a short pulse with enough energy fluence for MPD is used as shown by Black et al.[12] Then, excitation through the quasi-continuum to the dissocation level depends solely on energy fluence. This has been clearly demonstrated in a number of experiments.[12-14] Above the dissociation level, both the laser intensity and energy fluence can be important in the excitation process. In the case of long laser pulses with enough fluence, the energy fluence is sufficient to pump the molecules to a much higher excitation level above the dissociation energy, but the pumping is limited by depletion of population through dissociation. The average level of excitation or the average excess energy with which the molecules dissociate is then determined by the balance between the up-excitation rates and the dissociation rate. In other words, it is the laser intensity that determines the level of excitation at high energy fluence. In the case of shorter laser pulses, with not much fluence, the average level of excitation is limited by the available laser energy fluence. Even if the laser intensity is large enough that the up-excitation rate is much higher than the

dissociation rate, there is not enough energy fluence in the pulse to pump the molecules to higher levels. In the intermediate cases, the physical argument here suggests that both the laser intensity and the energy fluence should be important in determining the average level of excitation of SF_6 when it dissociates (see Fig. 15).

Our model calculations show that for SF_6 subject to a laser pulse with energy fluence below 5 J/cm^2 and intensity above 30 MW/cm^2, the average level of excitation is mainly determined by the energy fluence. This agrees with our experiment as shown in Fig. 17 where we compare the dissociation yields from laser pulses with energy fluence and peak intensity of 2.5 J/cm^2, ~200 MW/cm^2; 3 J/cm^2, ~60MW/cm^2; and 5 J/cm^2, ~100 MW/cm^2. If the laser intensity determines the excess energy in these cases, we would have found that the 2.5 J/cm^2 pulse results in the highest excess energy. Instead the 2.5 J/cm^2 pulse results in the smallest amount of excess energy. The excess energy predicted by the model calculation shown in Fig. 17 is in agreement with the experiment and shows that the excess energy should not depend appreciably upon the laser intensity until the energy fluence exceeds 5 J/cm^2.

These results contrast with the experiments presented in Ref. 19 where MPD was observed at energy fluences well above the threshold for dissociation. As expected, in those cases dissociation occurs at an excitation level where the up-excitation rate equals the dissociation rate determined by the laser intensity. In SF_6, this happens with our laser pulses with energy fluences > 10 J/cm^2 at 944 cm^{-1}. When the excitation level is limited by the laser intensity (and the

Fig. 17. Average number of excess photons absorbed by SF_6 beyond the dissociation threshold versus energy fluence. The experimental points are based on the agreement of the RRKM predicted angular distribution with the experimental angular distributions in Fig. 5. The laser pulses used were a 2.5 J/cm^2 laser shuttered pulse and 3 and 5 J/cm^2 normal pulses. The curves show the prediction of the model calculation ignoring half of the population with 3 excess photons and all population which dissociate with less than 3 excess photons, because the dissociation lifetime is longer than 10 μs.

———————— normal pulse

—— —— shuttered laser pulse

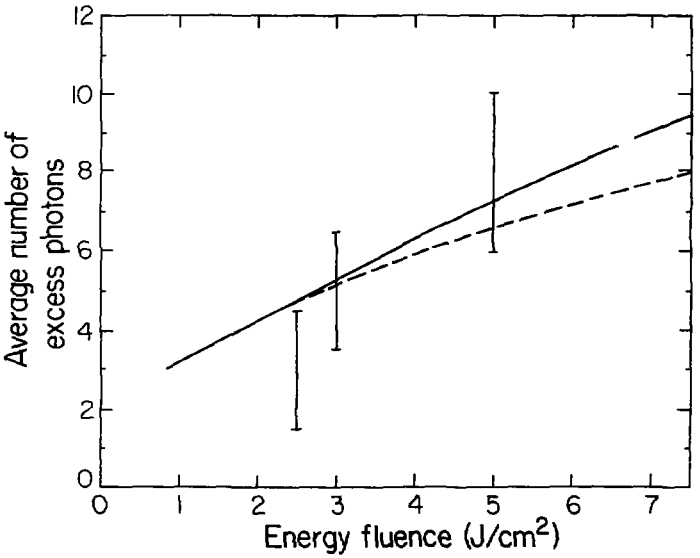

Fig. 17 XBL 795-1652

dissociation rate), significant dissociation will occur during the laser pulse. Then, the dissociation product can absorb more photons from the laser pulse and undergo a secondary dissociation. Thus, at higher laser fluences, the onset of secondary dissociation in SF_6 is closely associated with intensity-limited excitation. The conclusions for SF_6 should apply in general to MPD of other large polyatomic molecules.

CONCLUSION

In our experiments, the collisionless environment of the molecular beam enabled us to study many aspects of MPD of single, isolated molecules. In particular, we have investigated the effects of (1) initial vibrational excitation, (2) laser pulse duration, (3) laser energy fluence, and (4) laser frequency on the MPD of SF_6. These experiments provide quantitative results for the following processes in MPD: (1) intensity-dependent excitation over the discrete levels, (2) energy fluence dependent excitation in the quasi-continuum, and (3) excitation above the dissociation level including the subsequent dissociation dynamics.

The excitation over the discrete levels tends to limit the fraction of SF_6 molecules that can dissociate. This happens if the molecules have little initial vibrational excitation, if the laser pulse has a low intensity, or if the laser frequency is far off the peak of the linear absorption spectrum.

In the quasi-continuum more photons are absorbed by stepwise resonant excitations. Here, the excitation rate should be proportional to the laser intensity, but the average level of excitation for molecules in the quasi-continuum and the shape of the population distribution should depend only on the energy fluence. The absorption spectrum in the quasi-continuum broadens and shifts to lower energy as the excitation increases. In this way, the absorption cross section in the quasi-continuum, and hence the excitation rate, depends on the laser frequency.

The observed dissociation rates and the overall dissociation dynamics are in good agreement with predictions from the RRKM theory. The RRKM theory assumes that the excitation energy in a molecule randomly distributes in all vibrational modes in times much shorter than the dissociation lifetime. This assumption results in a dissociation rate constant that increases rapidly with increasing energy. At sufficiently high energy fluence, when molecules dissociate mostly during the laser pulse, the level from which molecules dissociate is limited by the laser intensity such that the up-excitation rate equals the dissociation rate. If the molecules dissociate after the laser pulse is over, it is because they are in excitation levels with long dissociation lifetimes, so that the excitation level is not determined by the competition of up-excitation and dissociation, but rather by the laser energy fluence. Thus, dissociation of molecules near the energy fluence threshold for observation of MPD occurs in general after the laser pulse is over.

In many gas cell experiments on SF_6 MPD, it has been assumed that the experiment is carried out under collisionless conditions if the laser pulse duration is shorter than the average collision time. Although this assumption is valid for the measurement of absorption, the dissociation yield is affected by collisions that occur after the laser pulse. SF_6 molecules that absorb one or two excess photons have a dissociation lifetime in the millisecond time regime; much longer than typical collision times in any experiment performed at low pressure. Consequently, the gas cell measurement of dissociation yields near the energy fluence threshold never occurs in a collisionless environment.

Although recently some people have expressed doubts concerning the similarities between SF_6 MPD and the MPD of other molecules, the experiments and model calculations described here elucidate dissociation characteristics generally applicable to the MPD of many other polyatomic molecules. Specifically, (1) at higher energy fluence the dissociation product often absorbs more energy to undergo secondary dissociation.[11,19,34] (2) Dissociation on the nanosecond timescale can be accurately modeled by the RRKM statistical theory.[19] (3) The absorption of infrared photons occurs via two steps: first an excitation over the discrete vibrational ladder and then excitation through the quasi-continuum.[1] Thus, a model calculation similar to the one we have presented here for SF_6 can also be applied to the MPD of many other polyatomic molecules. The experiments and model calculations show that though SF_6 multiphoton dissociation can be understood, experimental results are often rather complicated, depending on laser intensity, energy fluence, frequency, and molecular vibrational temperature.

REFERENCES

1. See the reviews:
V.S. Letokhov, and C. B. Moore, Sov. J. Quantum Electron., 6, 259; R. V. Ambartzumian and V. S. Letokhov in Chemical and Biochemical Applications of Lasers, Vol. 3, ed. C. B. Moore (Academic, New York, 1977), p. 166; N. Bloembergen and E. Yablonovitch, Physics Today, 31(5), 23 (May 1978); P. A. Schulz, Aa. S. Sudbø, D. J. Krajnovich, H. S. Kwok, Y.R. Shen and Y. T. Lee, Ann. Rev. Phys. Chem. in press (1979).

2. R.V. Ambartzumian, Yu A. Gorokhov, V. S. Letokhov, G. N. Makarov, and A. A. Puretzky, JETP Lett. 23, 22 (1976); Sov. Phys. JETP 44, 231 (1976).

3. R.V. Ambartzumian, Yu A. Gorokhov, V. S. Letokhov, G. N. Makarov, and A. A. Puretzky, JETP Lett., 23, 22 (1976); Sov. Phys. JETP 44, 231 (1976).

4. J.L. Lyman, R. J. Jensen, J. Rink, C. P. Robinson, and S. D. Rockwood, Appl. Phys. Lett., 27, 87 (1975).

5. K.C. Kompa, in Tunable Lasers and Applications, ed. A Mooradian, T. Jaeger, P. Stokseth (Springer, Berlin, 1976), p. 177.

6. M.J. Coggiola, P. A. Schulz, Y. T. Lee, and Y. R. Shen, Phys. Rev. Lett., 38, 17 (1977).

7. R.V. Ambartzumian, Yu A. Gorokhov, V. S. Letokhov, and G. N. Makarov, Sov. Phys. JETP 42, 993 (1975).

8. C.R. Quick, Jr. and C. Wittig, Chem. Phys. Lett., 48, 420 (1977).

9. J.M. Preses, R. E. Weston, Jr., and G. W. Flynn, Chem. Phys. Lett. 48, 425 (1977).

10. G.J. Diebold, F. Engelke, P. M. Lubman, J. C. Whitehead, and R. N. Zare, J. Chem. Phys., 67, 5407 (1977).

11. E.R. Grant, M. J. Coggiola, Y. T. Lee, P. A. Schulz, Aa. S. Sudbø, and Y. R. Shen, Chem. Phys. Lett., 52, 595 (1977).

12. J.G. Black, P. Kolodner, M. J. Shultz, E. Yablonovitch, and N. Bloembergen, Phys. Rev. A., 19, 704 (1979).

13. J.L. Lyman, and S. D. Rockwood, J. Appl. Phys. 47, 595 (1976).

14. J.G. Black, E. Yablonovitch, N. Bloembergen, and S. Mukamel, Phys. Rev. Lett., 38, 1131 (1977).

15. E.R. Grant, P. A. Schulz, Aa. S. Sudbø, Y. R. Shen, and Y. T. Lee, Phys. Rev. Lett., 40, 115 (1978).

16. J.L. Lyman, J. Chem. Phys., 67, 1868 (1977).

17. J. D. Lambert, D. G. Parks-Smith, and J. L. Stretton, Proc. Roy. Soc. A282, 380 (1964).

18. Y.T. Lee, J. D. McDonald, P. R. Le Breton, and D. R. Herschbach, Rev. Sci. Instu., 40, 1402 (1969).

19. Aa.S. Sudbø, P. A. Schulz, E. R. Grant, Y., R. Shen, and Y. T. Lee, J. Chem. Phys., 69, 2312 (1978).

20. P.J. Robinson and K. A. Holbrook, "Unimolecular Reactions" (Wiley, London, 1972); W. Forst. "Theory of Unimolecular Reactions" (Academic Press, New York, 1973).

21. M.J. Shultz, and E. Yablonovitch, J. Chem. Phys., 68, 3009 (1978).

22. H.S. Kwok and E. Yablonovitch, Phys. Rev. Lett., 411, 745 (1978).

23. M.C. Gower, and K. W. Billman, Opt. Commun., 20, 123 (1977).

24. F. Brunner, and D. Proch, J. Chem. Phys., 68, 4936 (1978).

25. A.V. Nowak, and J. L. Lyman, J. Quant. Spectrosc. Radiat. Transfer, 15, 945 (1975).

26. T. F. Bott, Appl. Phys. Lett, 32, 624 (1978).

27. Aa.S. Sudbø, P. A. Schulz, D. J. Krajnovich, Y. T. Lee, and Y. R. Shen, Opt. Lett., to be published.

28. R.V. Ambartzumian, N. P. Furzikov, Yu A. Gorokhov, V. S. Letokhov, G. N. Makarov, and A. A. Puretzky, JETP Lett., 23, 217 (1976); Opt. Commun., 18, 517 (1976).

29. W. Fuss, Chem. Phys., 36, 135 (1979).

30. D.M. Larsen, and N. Bloembergen, Opt. Commun. 17, 254 (1976).

31. H.W. Galbraith, and J. R. Ackerhalt, Opt. Lett., 3, 109 (1978); Opt. Lett., 3, 152 (1978); J. R. Ackerhalt and H. W. Galbraith, J. Chem. Phys., 69, 1200 (1978).

32. I.N. Knyazev, V. S. Letokhov, and V. V. Lobko, Opt. Commun., 25, 337 (1978).

33. I. Oref and B. S. Rabinovitch, Acc. Chem. Res., 12, 166 (1979).

34. J. D. Campbell, M. H. Yu, and C. Wittig, Appl. Phys. Lett. 32, 413 (1978); J. D. Campbell, M. H. Yu, M. Mangir, and C. Wittig, J. Chem. Phys. 68, 3854 (1978).

III. ROLES OF LASER INTENSITY AND ENERGY FLUENCE IN A MODEL CALCULATION FOR MULTIPHOTON DISSOCIATION

INTRODUCTION

Multiphoton dissociation (MPD) of polyatomic molecules has been studied extensively in recent years. Many results have elucidated the fundamental mechanisms involved in the process, but others seem to have confused the issues because the important roles played by both laser intensity and energy fluence (i.e., the time integrated intensity) in multiphoton dissociation have not been fully appreciated. The well-accepted veiw of multiphoton dissociation is that the initial excitation over the discrete levels should depend on the laser intensity, but the excitation in the quasi-continuum is controlled by the laser energy fluence. Beyond the dissociation energy, up-excitation may compete with dissociation and then the level of excitation and the rate of dissociation depend on the laser intensity. The effects of laser intensity are however often disregarded when interpreting the experimental results; more attention has been paid to the effects of energy fluence. Thus, for example, recent results by Brenner[1] indicating that products from MPD of ethyl vinyl ether are different when the laser intensity is varied but the energy fluence is kept constant, have led to speculations of a mode controlled chemical decomposition. This interpretation is not valid because it ignores the effect intensity has on the average level of excitation of dissociating molecules.

In this paper the effects that laser intensity and energy fluence have on multiphoton excitation, dissociation, and the excess energy (i.e., energy beyond the dissociation energy) with which the molecules dissociate are carefully examined using a realistic model calculation which was developed recently[2] based on experimental observations. We select parameters which are indicative of multiphoton dissociation of SF_6 and CF_3I for illustration and comparison. SF_6 is selected because its multiphoton dissociation behavior is the best understood of all molecules. CF_3I is chosen as a contrast to SF_6 because the dissociation rate for CF_3I is much larger than for SF_6 given the same excess energy. The competition between up-excitation and dissociation limits the energy absorbed by a CF_3I molecule to just a little (0.1 eV) more than the dissociation energy, whereas SF_6 can absorb a lot (1 eV) more than the dissociation energy under the same conditions. Changes in the multiphoton dissociation behavior may also be expected as the frequency is varied, so model calculations wer also performed to simulate the frequency dependence of the SF_6 dissociation yield. Finally, the effects of collisions in multiphoton dissociation experiments are briefly discussed.

PHYSICAL DESCRIPTION OF MPD

During the past five years, it has been found useful to consider three separate regimes in the multiphoton excitation and dissociation process:[3] (1) the intensity-dependent excitation over the low lying discrete states, (2) the energy fluence-controlled excitation in the quasi-continuum, and (3) the excitation in the dissociative continuum from which molecules dissociate at a rate that depends upon the level of excitation.

In the first regime, molecules with little initial internal energy are excited over the discrete states into the quasi-continuum by an intensity-dependent, nearly resonant multiphoton absorption process. Molecules in different rotational-vibrational states have different resonant frequencies and therefore are subject to different intensity dependences. Although the detailed excitation mechanism in the discrete states is complicated, as a rule higher laser intensities will excite a larger fraction of the molecules into the quasi-continuum.

Once the molecules are in the quasi-continuum they can be further excited by resonant, stepwise single photon transitions. As long as relaxation of the excitation is negligible, this is possible even at low laser intensities. The intensities in typical experiments, though higher than necessary, are low enough that nonlinear absorption in the quasi-continuum is probably unimportant. Then, the rates of absorption and stimulated emission are linear in the laser intensity,

and the net absorption or molecular excitation in this region is a function only of the laser energy fluence.

Above the dissociation energy, resonant stepwise single photon transitions still dominate the excitation process, but now molecular dissociation competes with up-excitation. This competition has no effect on the total dissociation yield. However, it can affect the level of excitation of molecules that dissociate during the laser pulse, because the up-excitation rate is proportional to the laser intensity, while the dissociation rate depends on the level of excitation. Recent molecular beam results[4] have shown that RRKM calculations can be used to deduce the dissociation rate constants of multiphoton excited molecules. The dissociation rate constants increases with increasing excess energy. For SF_6 excited to 0.1 eV above the dissociation energy of 4.0 eV,[5] the dissociation lifetime (i.e., the reciprocal of the rate constant) is 10 ms, which is much longer than the typical TEA CO_2 laser pulse duration of 100 ns. Then, dissociation occurs mostly after the laser pulse is over. This happens whenever the available energy fluence limits the up-excitation. With higher energy fluence, the level of excitation can be higher and for a constant laser intensity, is eventually limited by the rapidly increasing dissociation rate constant. In this high fluence experiment, an increase in laser intensity (while keeping the energy fluence unchanged) will excite the molecule to a higher energy level until the dissociation rate again approximately equals

the up-excitation rate. This happens, for example, for SF_6 excited by a 100 ns, 10 J/cm^2 TEA CO_2 laser pulse; dissociation and up-excitation rate constants are both about 0.1/ns with dissociation occurring from an average level around 10 photons (1.2 eV) above the dissociation level.

This description of MPD can be incorporated into a rate equation model which has been discussed and developed in the literature.[2,5-8] The major assumptions in this model[2] are: (1) the fraction of molecules excited to the quasi-continuum is only a function of laser intensity (see Fig. 1) and (2) the evolution of population in the quasi-continuum is given by:

$$\frac{dN_m}{dt} = \frac{I(t)}{h\nu}\left[\sigma_{m-1}N_{m-1} + \frac{g_m}{g_{m-1}}\sigma_m N_{m+1} - \left(\sigma_m + \frac{g_{m-1}}{g_m}\sigma_{m-1}\right)N_m\right] - k_m N_m$$

where $h\nu$ is the energy of a photon, N_m is the fraction of population with internal energy $mh\nu$ (m = positive integers), g_m is the density of states at the energy $mh\nu$, $I(t)$ is the laser intensity, k_m is the RRKM dissociation rate constant for molecules with internal energy $mh\nu$, and σ_m is the absorption cross section for molecules with internal energy $mh\nu$. The values of σ_m and f, the fraction of molecules excited to the quasi-continuum as a function of intensity, were obtained empirically by comparison with experiments of Black et al.,[9] as described previously.[2] We found the function f shown in Fig. 1

Fig. 1. The fraction of molecules that have entered the quasi-continuum as a function of laser intensity. It is assumed that molecules, once excited to the quasi-continuum never reenter the discrete states.

$$f = \frac{1}{\sqrt{\pi}} \int_{-\infty}^{\gamma \ln I/I_0} e^{-x^2} dx$$

$$\gamma = 0.5; \quad I_0 = 20 \text{ MW/cm}^2$$

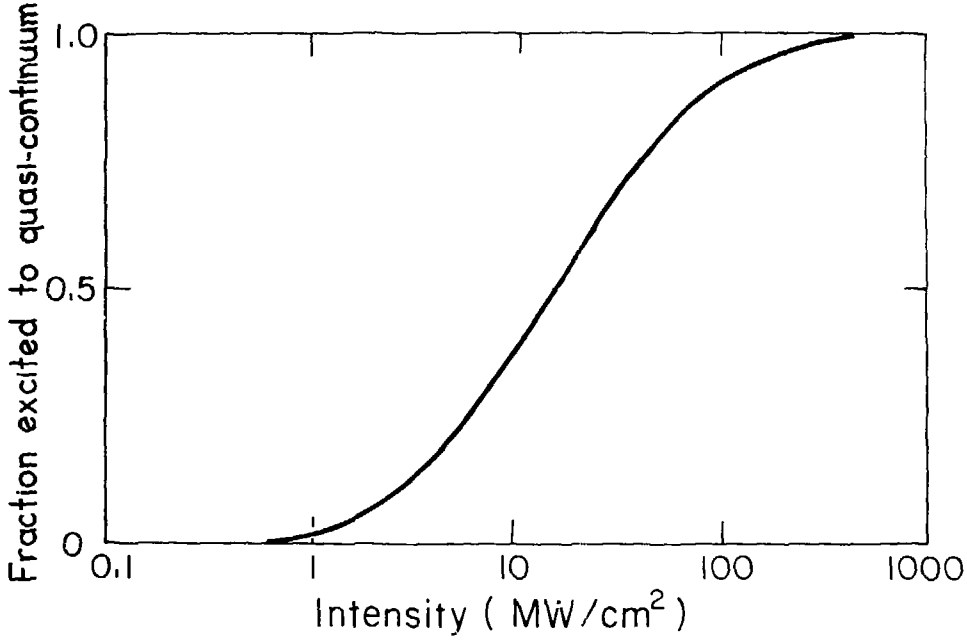

Fig. 1

XBL799-2968A

and $\sigma_m = \sigma_o e^{-\beta m}$ with $\sigma_o = 8 \cdot 10^{-19}$ cm^2, $\beta = 0.042$. We assume in this paper that the laser intensities required to excite CF_3I to the quasi-continuum and σ_m for CF_3I are identical to those for SF_6.

In making the comparison with the experiments of Black et al.,[9] the average number of photons absorbed must be defined in terms of the calculated population distribution. The average number of photons absorbed, $\langle n \rangle$, is the weighted average of the number of photons absorbed for molecules that have entered the quasi-continuum and the number of photons absorbed for molecules in the discrete states:

$$\langle n \rangle = f\langle n \rangle_{QC} + (1-f)\langle n \rangle_{DS}$$

where $\langle n \rangle_{QC}$ is the average level populated in the quasi-continuum, and $\langle n \rangle_{DS}$ is the average number of photons absorbed by molecules that remain in the discrete states. $\langle n \rangle_{DS}$ cannot be derived from this model calculation, so to obtain $\langle n \rangle$, we assume that $(1-f)\langle n \rangle_{DS} \ll f\langle n \rangle_{QC}$. At low laser intensities and energy fluences this assumption breaks down because a large fraction of molecules remain in the discrete states. This has been confirmed by photoionization experiments on multiphoton excited SF_6.[10] The assumption $(1-f)\langle n \rangle_{DS} \ll f\langle n \rangle_{QC}$ is valid at higher laser intensity (since f is larger) and/or at higher energy fluence (since $\langle n \rangle_{QC}$ is larger). At even higher intensities, all the molecules are excited to the quasi-continuum, so $\langle n \rangle = \langle n \rangle_{QC}$. The indiscriminate use of the equation $\langle n \rangle = \langle n \rangle_{QC}$

has however led to the erroneous analysis of the effective vibrational temperature and to the conclusion of a mode selective decomposition.[11]

The effects of laser intensity and energy fluence on MPD of SF_6 and CF_3I differ only because the CF_3I dissociation energy is smaller and its dissociation rate constants are larger for a given level of excitation. Changes in the MPD behavior may also appear in the model calculation due to changes in the fraction excited to the quasi-continuum and the quasi-continnum cross section. Such changes may arise from laser frequency variations. Accordingly, the roles of laser intensity and energy fluence change slightly, though the principles discussed remain valid.

The physical explanation for changes in the fraction excited to the quasi-continuum with frequency is that as the frequency is tuned away from the fundamental frequency at the same laser intensity, fewer molecules in the spread of initial rotational states can be resonantly or near resonantly excited, and thus fewer molecules enter the quasi-continuum. Higher laser intensities are then required to pump into the quasi-continuum those molecules in states not near resonances.[12]

For SF_6, there is also evidence that the absorption cross section in the quasi-continuum, in addition to the fraction of molecules entering the quasi-continuum, depends on the laser frequency. If the SF_6 molecules have significant internal energy, anharmonicity causes the absorption spectrum to shift to lower frequency and become

broader. Thus, the quasi-continuum cross section decreases with increasing internal energy at frequencies near the peak of the linear absorption spectrum (~944 cm^{-1}). At frequencies below the linear peak absorption, the cross section is small for molecules with little internal energy, but increases with increase of internal energy. This qualitative picture has been confirmed by the multiphoton dissociation experiments of Gower and Billman[13] and this group,[2] which show that the energy fluence threshold for dissociation of SF_6 is lower at 930 cm^{-1} than at higher frequency, even though the maximum absorption occurs at 944 cm^{-1}.

MODEL CALCULATIONS

A. $\langle n \rangle$ and Dissociation Yield

For many polyatomics such as SF_6 and CF_3I the peak intensity of a 100 ns TEA CO_2 laser pulse focused to several joules per square centimeter is sufficient to excite almost all of the population to the quasi-continuum and $\langle n \rangle = \langle n \rangle_{QC}$. When this is the case, the model predicts and experiments[13-15] have confirmed that the energy fluence alone determines the average level of excitation in the quasi-continuum and the total dissociation yield. The dependence of the multiphoton excitation solely on energy fluence has been discussed in previous model calculations[5,6,9] that ignore the presence of an intensity-dependent excitation over the discrete states. Such a model, as well as this model at intensities high enough to excite all molecules to the quasi-continuum, predicts a quasi-continuum population distribution for the molecules that depends only on the laser energy fluence.

Figure 2 shows the population distribution obtained from our model calculation for various energy fluences assuming that the laser intensity is high enough to excite all molecules to the quasi-continuum. It is clear from Fig. 2 that an increase in the energy fluence pumps the quasi-continuum population to higher levels and causes a spreading of the population distribution. According to the model, even at laser intensities too low to excite all of the molecules to the quasi-continuum, the population distribution of

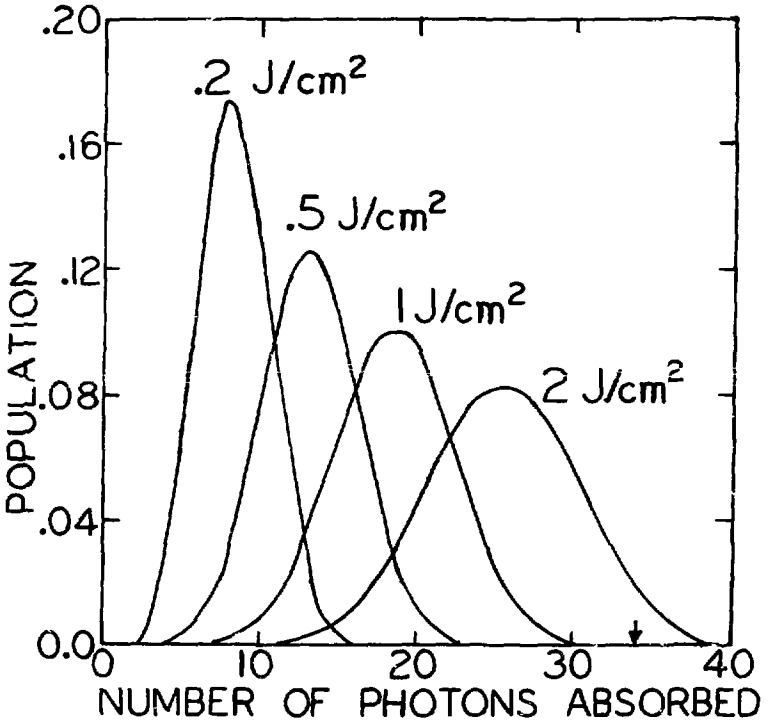

XBL 7910-12103

Fig. 2. Population distribution in the quasi-continuum assuming the laser intensity is high enough that all molecules are excited to the quasi-continuum. Although a Gaussian laser pulse of 1 ns duration is used, the population distribution is independent of laser pulse shape and duration. Therefore, the curves are labeled only by the energy fluence. The first dissociative level is marked by the arrow.

those molecules in the quasi-continuum is still determined by the energy fluence. At sufficiently high fluence, the high energy tail of the distribution extends above the dissociation level and the molecules start to dissociate.

Figure 3 shows the relation between <n> and energy fluence at various constant laser intensities for SF_6 and CF_3I. At the highest intensity (2 GW/cm^2), essentially all of the molecules are excited to the quasi-continuum (see Fig. 1), so <n> = $<n>_{QC}$. Consequently, <n> depends only on energy fluence. At the lower laser intensities, <n> (= f$<n>_{QC}$) increases with either increasing intensity (increasing f) or energy fluence (increasing $<n>_{QC}$). At 200 MW/cm^2 95% of the SF_6 is excited to the quasi-continuum, so there is a 5% decrease in <n> when lowering the peak intensity from 2 GW/cm^2 to 200 MW/cm^2 for the same energy fluence. At 20 MW/cm^2 only half the molecules are excited to the quasi-continuum so <n> is only half as large as <n> at 2 GW/cm^2 and the same energy fluence.

The model calculation prediction of <n> versus energy fluence for CF_3I is almost identical to the corresponding SF_6 result at low energy fluence (as it should be since the model parameters were chosen to be the same), but then falls off at higher energy fluence. At higher fluence than shown in Fig. 3, a similar fall-off may be expected in the SF_6 curve. The <n> falls off when the energy fluence becomes large enough to cause dissociation, because <n> is defined in the model calculation to include only the internal energy in the

Fig. 3. <n> in SF_6 versus laser energy fluence shown by the solid curves for three different laser intensities. The <n> is obtained from the model calculation using a laser pulse with a Gaussian time dependence and a peak laser intensity of:

○ 2000 MW/cm^2

● 200 MW/cm^2

◊ 20 MW/cm^2

The dashed curve gives <n> in CF_3I versus energy fluence for a peak laser intensity of 200 MW/cm^2.

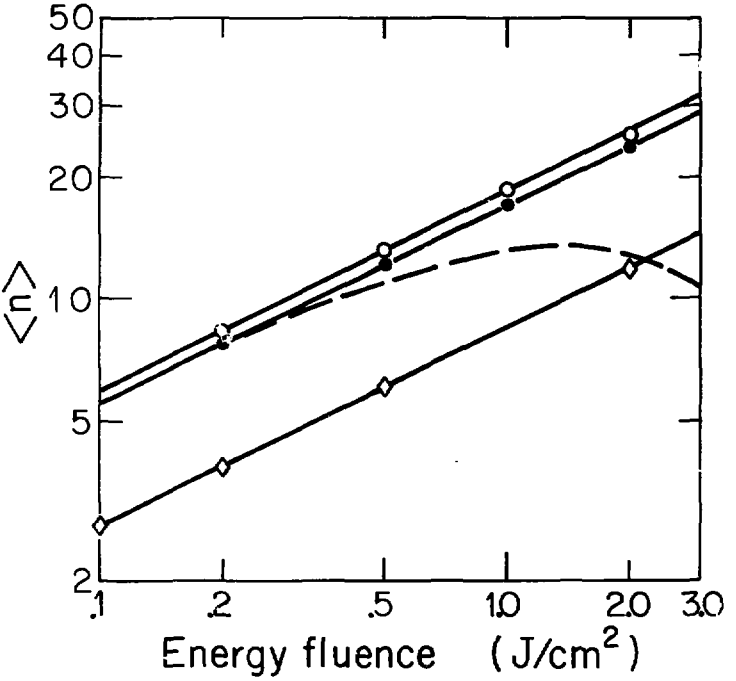

XBL799-2969

Fig. 3

molecule. When the molecules dissociate the internal energy equal to the dissociation energy is used up in breaking the chemical bond. The particular definition of <n> used for this model calculation is chosen because an opto-acoustic measurement of <n> is sensitive to the translational and internal energy of the molecules. Thus, the opto-acoustic experimental results should agree with the <n> predicted by the model provided that in the experiment the fragments do not recombine or release energy by further reaction. In the model calculation, the <n> for CF_3I falls off at lower energy fluence than SF_6 because CF_3I dissociates at a lower energy fluence than SF_6 (to be discussed later). The actual experimental measurement of <n> for SF_6 is further complicated by SF_5 absorption which tends to counteract the decrease in <n> with increasing energy fluence.

The total dissociation yield, as we have already mentioned, increases with energy fluence. The dissociation yield, according to the model, also increases with increasing laser intensity, because the fraction of molecules in the quasi-continuum is then larger. However, the normalized dissociation yield, which is the total dissociation yield divided by the fraction of molecules that do reach the quasi-continuum depends only on the energy fluence. This is demonstrated in Fig. 4 which shows the normalized dissociation yield for SF_6 and CF_3I versus energy fluence for several constant laser intensities. Figure 4 also shows that CF_3I dissociates at a lower energy fluence than SF_6 though they have absorbed the same

Fig. 4. Normalized dissociation yield versus energy fluence for SF_6 at four different laser intensities and for CF_3I at 200 MW/cm^2. The normalized dissociation yield is the dissociation yield divided by the fraction of molecules that have entered the quasi-continuum. At high energy fluence all molecules that have entered the quasi-continuum dissociate.

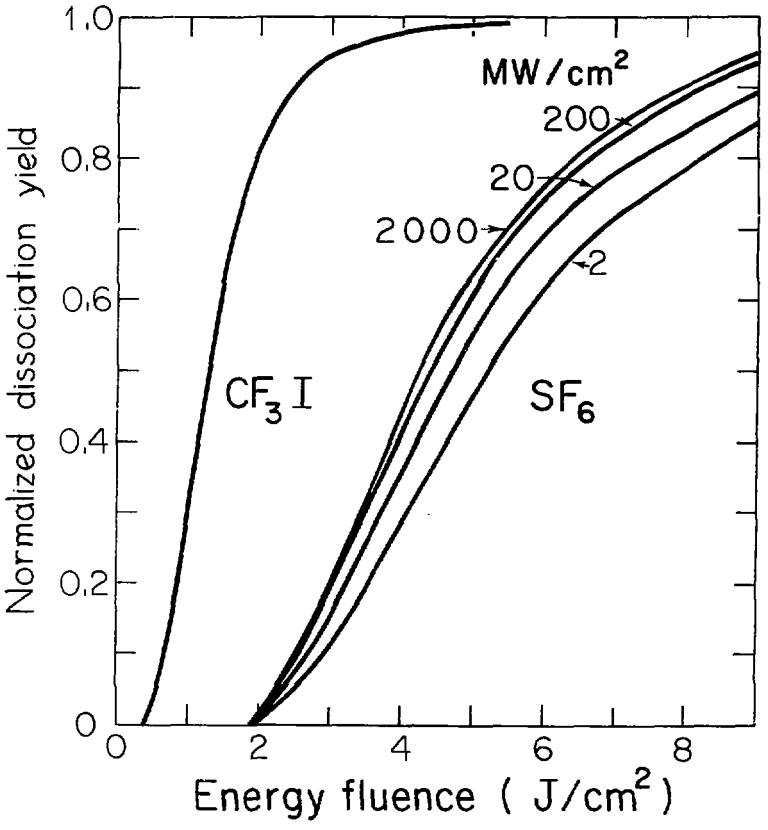

XBL 799-2971A

Fig. 4

number of photons, because CF_3I has a much lower dissociation energy (2.2 versus 4.0 eV). The slight intensity dependence in Fig. 4, which is most pronounced at low intensity, comes about because molecules that initially require a high laser intensity to be excited to the quasi-continuum are not excited to the quasi-continuum until the middle of the Gaussian laser pulse when the peak laser intensity is achieved. Molecules are then subject to different amounts of energy fluence depending on when they entered the quasi-continuum.

B. Excess Energy

The excess energy with which molecules dissociate can be limited by the amount of up-excitation (energy fluence controls the excess energy) or by the competition between the up-excitation and the dissociation (intensity controls the excess energy). Figure 5 shows the model calculation of excess energy with which SF_6 and CF_3I dissociate as a function of laser energy fluence. CF_3I mostly dissociates with very little excess energy independent of energy fluence. Even at very high intensities CF_3I is not excited much beyond its dissociation energy, because the dissociation lifetime of CF_3I is very short (only 1 ns at one photon above the dissociation limit) and rises rapidly with increasing excess energy. In general, the energy fluence controls the excess energy when the dissociation lifetimes for the energy levels populated are longer than the laser pulse duration. Thus, energy fluence control of the excess energy in CF_3I occurs only for very high laser intensities and low energy fluences. On the other hand, the excess energy of SF_6 is controlled by the energy fluence at energy fluences below 10 J/cm^2 and for a peak laser intensity of 2000 MW/cm^2, and at lower energy fluences for the lower laser intensities. At higher energy fluences (for a constant intensity) SF_6 is excited to higher internal energies where the competition between up-excitation and dissociation, and thus the intensity, determines the amount of excess energy deposited in the molecule at dissociation. This is shown in Fig. 5 by a saturation of the excess energy for a given laser intensity.

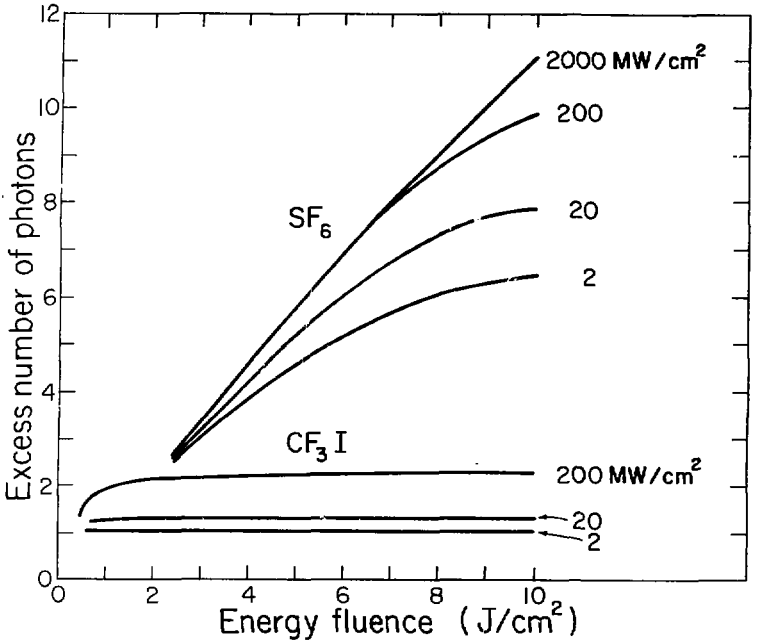

XBL799-2970

Fig. 5. Excess energy with which CF_3I and SF_6 dissociate for several peak laser intensities and energy fluences below 10 J/cm^2.

The actual distribution of excess energies with which SF_6 dissociates, calculated from the model and shown in Fig. 6, is considerably broader when energy fluence limits the excess energy (5, 0.5, and 0 ns pulses) than when intensity controls the excess energy (50-5000 ns pulses). For the short laser pulses most of the molecules dissociate after the end of the laser pulse (shown by the dashed curves). The broad distribution of excess energies then reflects the spread in that part of the population distribution beyond the dissociation energy at the end of the laser pulse. On the other hand, for longer laser pulses, when the excess energy is controlled by the laser intensity, the molecules dissociate during the laser pulse from only a few levels where the up-excitation rate approximately equals the dissociation rate.

Experimental results are also becoming available on the time resolved production of MPD products.[16] Therefore, we use the model calculation to investigate when the dissociation products are formed and with how much excess energy. Figure 7 shows the time dependence of the rate of dissociation (i.e., the number of molecules dissociated per unit time for a given level) of SF_6 that has absorbed 5, 7, 10, and 12 excess photons. The SF_6 is illuminated by a 60 ns FWHM 7.5 J/cm^2 laser pulse with a shape typical of many TEA CO_2 laser pulses, having a 300 ns tail containing 40% of the total energy fluence. After the energy fluence threshold for dissociation is reached (at 80 ns), SF_6 with 5 excess photons dissociates at a nearly constant

Fig. 6. Model calculations varying the peak laser intensity of a Gaussian laser pulse at a constant 10 J/cm^2, to illustrate the role of laser intensity. At low laser intensity (5000 and 500 ns pulses), the fraction excited into the quasi-continuum limits the dissociation yield. Intensity limits the average excess energy for the 5000, 500, and 50 ns laser pulses. Energy fluence limits the average excess energy for the 5, 0.5, and 0 ns laser pulses. Most molecules then dissociate after the laser pulse, as shown by the dashed curves. In the limit of 0 ns all molecules dissociate after the laser pulse.

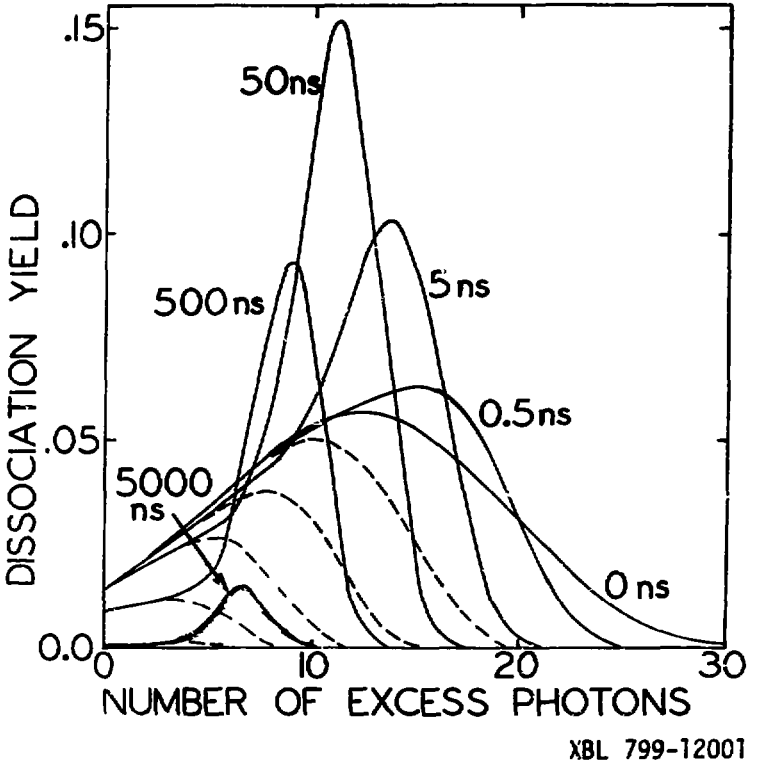
.15
.10
.05
0.0
DISSOCIATION YIELD
50ns
500ns
5ns
0.5ns
5000
ns
0 ns
0
10
20
30
NUMBER OF EXCESS PHOTONS
XBL 799-12001

Fig. 6

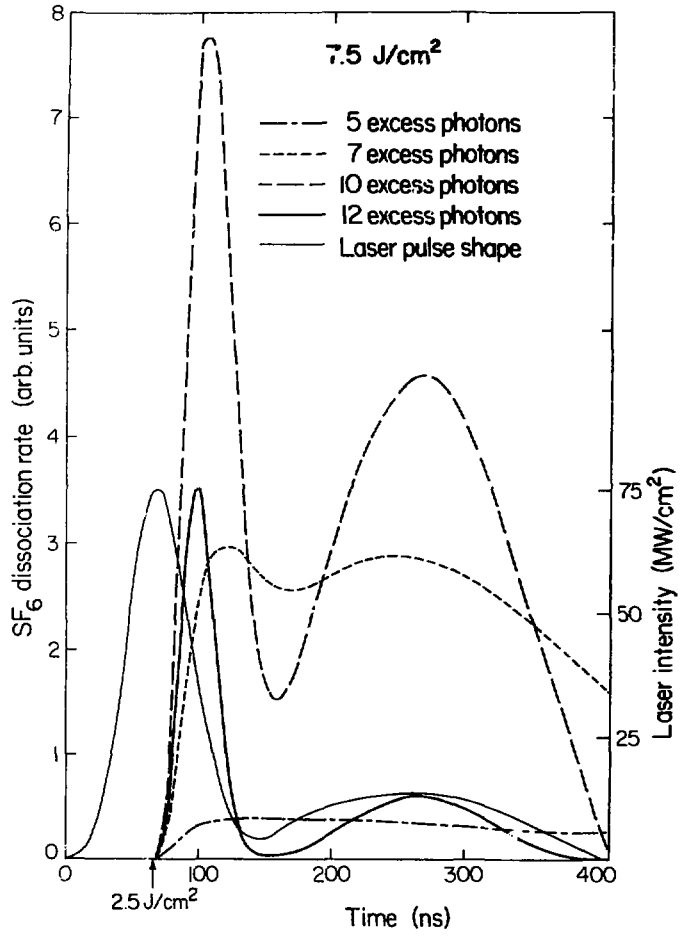

XBL 795-1656

Fig. 7. Excess energies with which SF_6 dissociates versus time. The CO_2 TEA laser pulse used in this model calculation is shown by the light solid curve with the intensity scale shown on the right.

rate for the remainder of the laser pulse. The constant rate of dissociation is a consequence of the relatively long lifetime (~1 μs) for SF_6 with 5 excess photons and of a steady state equilibrium for laser pumping into and out of this level. Dissociation from levels of higher excess energy and correspondingly larger dissociation rate constants tends to occur during the time of high laser intensity when the up-excitation rate is high. This becomes especially evident in the case of 12 excess photons.

To summarize, Fig. 8 shows whether the laser intensity or the energy fluence controls the excess energy in the model calculation for a Gaussian laser pulse. The parameter which controls the excess energy depends on the values of the laser intensity and energy fluence and also on the molecule. For instance, the excess energy of SF_6 excited by a 100 ns laser pulse (dashed curve), is limited by the energy fluence for fluences below approximately 8 J/cm^2 and by the laser intensity at higher energy fluences. Actually, the transition from energy fluence to intensity control of the excess energy occurs gradually as shown in Fig. 5, not quickly, as implied by the line separating the two regions in Fig. 8. For CF_3I a third region appears where the excess energy is independent of both laser intensity and energy fluence, because the dissociation lifetime just one photon above the dissociation limit is so short that the moelcules dissociate before they can absorb another photon. So the excess energy becomes independent of the energy fluence and

Fig. 8. Parameter determining the amount of excess energy with which (a) SF_6 and (b) CF_3I dissociate using a Gaussian laser pulse with a peak laser intensity given on the ordinate and an energy fluence given on the abscissa. In the region labeled energy fluence, the energy fluence limits the excess energy with which the molecules dissociate. In the region labeled intensity the competition between up-excitation and dissociation limits the excess energy. Below 30 MW/cm^2, most CF_3I dissociates after absorbing just enough photons to exceed the dissociation energy, as discussed in the text. The dashed curve gives the relationship between peak laser intensity and energy fluence for a Gaussian laser pulse with a duration of 100 ns FWHM. A line is drawn where 0.01% of the molecules dissociate.

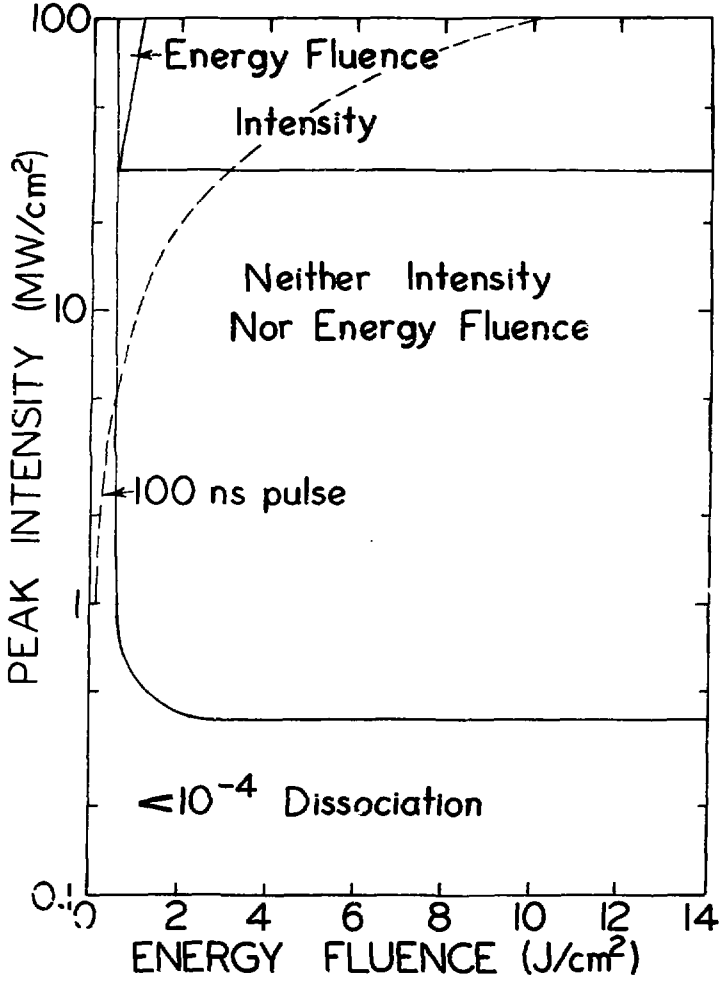

XBL 799-12003

Fig. 8(a)

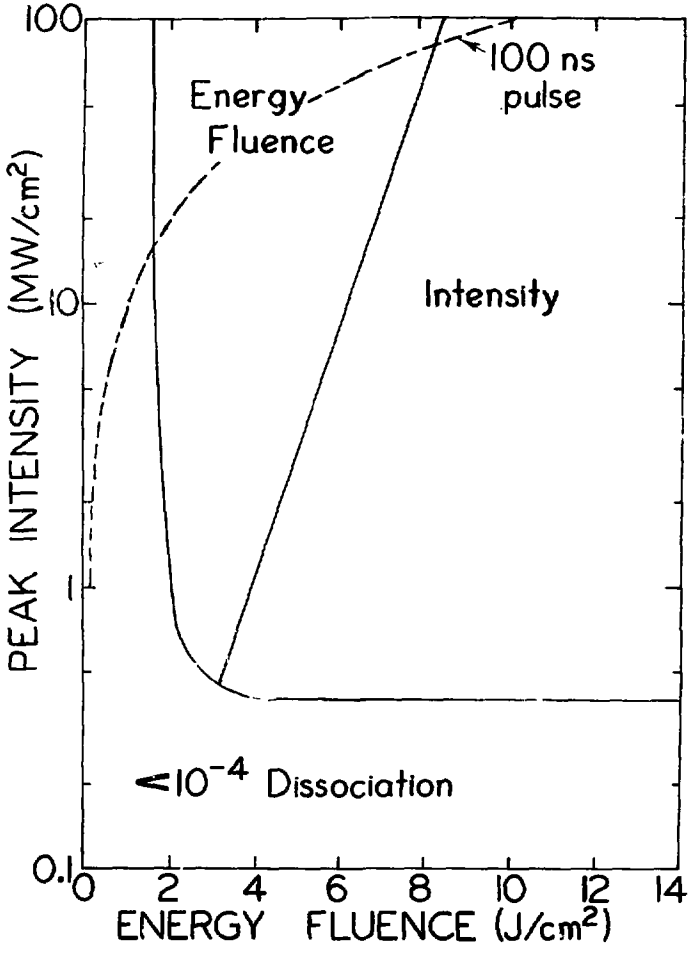

XBL 799-12004

Fig. 8(b)

intensity and, if a single photon can excite the molecule from a level where the up-excitation rate is much larger than the dissociation rate to a level where the up-excitation rate is much smaller than the dissociation rate, which is the case for CF_3I excited by a CO_2 laser.

Figure 9 also shows the minimum laser intensities and energy fluences required to observe 0.01 dissociation in SF_6 and CF_3I. For SF_6 illuminated by a laser pulse of 100 ns or shorter duration, 0.01 dissociation is observed at approximately 1.8 J/cm^2. This is the energy fluence threshold for SF_6 predicted by the model calculation and agrees with experimental results.[13,15] On the other hand, when the energy fluence is larger than 4 J/cm^2 and the laser pulse duration is longer than 10 μs, the model predicts a peak laser intensity threshold of approximately 0.4 MW/cm^2 required for 0.01 dissociation of SF_6.

C. Frequency

Frequency variations cause changes in the fraction of molecules excited to the quasi-continuum and in the quasi-continuum cross section. Thus, it is not surprising that the results of molecular beam experiments[2] on the energy fluence dependence of the dissociation yield change with frequency. Figure 9 shows the dissociation yield versus energy fluence obtained using different parameters in the model calculation in order to accurately simulate the experimental results at different frequencies. The experiments were carried out using multimode laser pulses with the pulse shape given in Fig. 7. As was done in Ref. 2, the peak laser intensity in a multimode pulse is assumed to be twice the peak laser intensity of a single mode pulse. The parameters used in the model to fit the data are given in the caption of Fig. 9, but due to the lack of complementary data at frequencies other than 944 cm^{-1}, the parameters are not as accurate at the other frequencies as at 944 cm^{-1}. Nevertheless, the experimental data allows us to draw the following conclusions in the context of the model. First, the laser intensity required to excite SF_6 molecules at 300 K to the quasi-continuum is a minimum near 944 cm^{-1} and is approximately an order of magnitude higher at the frequencies 935 cm^{-1} and 953 cm^{-1}. Second, the average quasi-continuum cross section decreases by approximately a factor of two for every 10 cm^{-1} increase in frequency between 935 cm^{-1} and 953 cm^{-1}.

Fig. 9. MPD yield of SF_6 versus energy fluence for a multimode laser pulse with the shape shown in Fig. 7. The parameters of both the bottleneck and the quasi-continuum cross section have been adjusted (except for 944 cm^{-1}) to give a good fit to the data. The normalization factor is obtained by scaling the yield at 944 cm^{-1} to obtain a good fit.

— — 935 cm^{-1} $\gamma = 0.5$ $I_0 = 400$ MW/cm^2 $\sigma_0 = 16 \cdot 10^{-19}$ cm^2 $\beta = 0.026$

——— 944 cm^{-1} $\gamma = 0.5$ $I_0 = 20$ MW/cm^2 $\sigma_0 = 8 \cdot 10^{-19}$ cm^2 $\beta = 0.042$

— – — 953 cm^{-1} $\gamma = 0.5$ $I_0 = 400$ MW/cm^2 $\sigma_0 = 4 \cdot 10^{-19}$ cm^2 $\beta = 0.035$

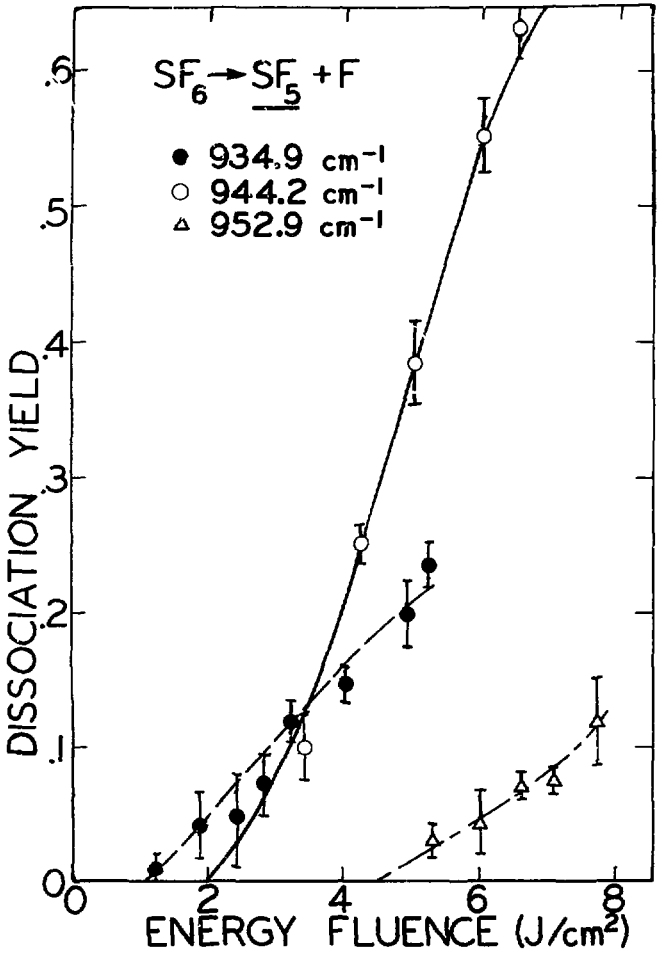

XBL 799-11999

Fig. 9

In the model calculation the fraction excited to the quasi-continuum and the quasi-continuum cross section affect <n> and the dissociation yield, though only the quasi-continuum cross section affects the average excess energy with which molecules dissociate. Therefore it should be expected that <n>, dissociation yield, and excess energy are all functions of frequency. Figure 10 gives the model calculation prediction of the excess energy with which SF_6 dissociates as a function of energy fluence at three different frequencies, using the same parameters as in Fig. 9. At energy fluences below 4 J/cm^2 the energy fluence limits the excess energy for all three frequencies. The larger average quasi-continuum cross section at the low frequencies causes the molecules to be excited further in the quasi-continuum, so the average excess energy with which the SF_6 dissociates is larger. Above 15 J/cm^2 the up-excitation is high enough that dissociation competes with further up-excitation for all the frequencies. Then the laser intensity controls the excess energy, and the excess energy is greatest for the frequency (935 cm^{-1}) where the cross section at the dissociation levels, and hence the up-excitation rate, is largest.

Fig. 10. Prediction of excess energy of SF_6 in multiphoton dissociation versus energy fluence for three different frequencies. The model calculation is the same used for Fig. 9.

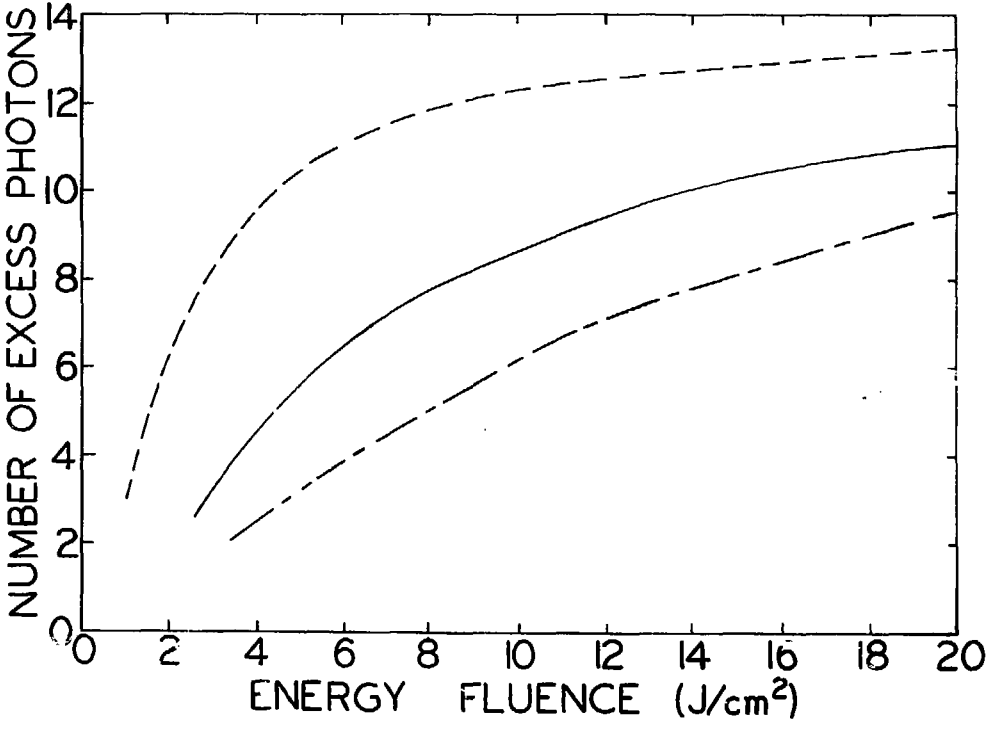

Fig. 10

XBL 799-12000

DISCUSSION

Because the laser intensity and energy fluence affect the excess energy with which molecules dissociate, these parameters also determine the dissociation channel. Molecules with large dissociation rate constants for low excess energies generally dissociate along the lowest dissociation energy channel. A higher dissociation energy channel may be observed if the excess energy is great enough, which tends to occurs for larger molecuels with dissociation rate constants which increase more slowly with excess energy. The ratio of products appearing in several dissociation channels is determined by the distribution of excess energies and by the ratio of the dissociation rate constants into the different channels from each level. When energy fluence limits the excess energy, increasing the energy fluence increases the average amount of excess energy and makes observation of a higher dissociation energy channel more likely. A model calculation for C_2F_5Cl predicts that multiphoton dissociation into the lower energy channel, $C_2F_5 + Cl$, dominates at low energy fluence. At high energy fluence, the higher energy channel, $CF_3 + CF_2Cl$, assumes a larger fraction of the dissociation yield. This has actually been observed in a molecular beam experiment.[17]

If, instead of energy fluence, the intensity controls the amount of excess energy, then changing the energy fluence at constant laser intensity should not change the excess energy or the ratio of dissociation products. However, increasing the intensity at constant

energy fluence increases the excess energy and thus can change the dissociation products. This may explain the observation of two different dissociation channels from ethyl vinyl ether at two different intensities using the same energy fluence.[1] Competition between several dissociation channels thus provides a stringent test of the model calculation's ability to predict excess energy.

Because the quasi-continuum cross section may depend on frequency, a change in the laser frequency at identical laser energy fluence and intensity can affect the dissociation product. Thus, experiments showing that the dissociation products depend on the laser frequency,[18] which have been used to defend the mode selective hypothesis, could be a result of a dependence of the quasi-continuum cross section on frequency. A change in the fraction excited to the quasi-continuum and not the cross section, accomplished, for instance, by changing the initial molecular temperature, does not change the excess energy, so the results of such experiments are more easily interpretable, as was shown in the results of molecular beam experiments.[2]

Collisions, like the frequency, have more than one effect on multiphoton dissociation. The fraction of molecules excited to the quasi-continuum is increased by collisional hole filling of states that have been depleted by excitation to the quasi-continuum. This has already been included in a rate equation model[16] and should, now that it is generally recognized, cause no further problems in

interpretation. However, in addition, collisions alter the ensemble population distribution toward a thermal, Boltzman population distribution with the same value of <n>. Despite the constancy of <n>, the altered population distribution means that collisions can change both the dissociation yield and the excess energy with which molecules dissociate. Therefore, collisions can be ignored in measuring the dissociation yield only if the molecules with enough energy to dissociate do so before collisions occurs. For example, SF_6 excited just above its dissociation threshold has lifetimes for dissociation much longer than the laser pulse duration and may be collisionally deactivated even long after the end of the laser pulse.

CONCLUSION

An empirical rate equation model consistent with experimental results on MPD, shows that at very high laser intensities the laser energy fluence controls the amount of excitation. At lower intensities an intensity-dependent fraction of the molecules are excited to the quasi-continuum where the excitation is still determined by the energy fluence. This model is used to predict $\langle n \rangle$, dissociation yield and excess energy dependences on laser intensity and energy fluence. The average number of photons absorbed by molecules and the dissociation yield are determined by the peak laser intensity, because the intensity controls the fraction of molecules excited to the quasi-continuum, and the energy fluence, because fluence controls the net amount of excitation for molecules that have been excited to the quasi-continuum. The excess energy with which molecules dissociate is limited by the energy fluence when the dissociation occurs after the laser pulse and by the intensity when the dissociation competes with the up-excitation during the pulse.

We have treated both SF_6 and CF_3I as examples of MPD in large and small molecules. They differ by the way intensity and energy fluence determine the excess energy with which the molecules dissociate. For a small molecule with a small dissociation energy, the dissociation rate constant increases extremely rapidly with excess energy and the molecules dissociate with little excess energy for typical laser intensities. For large molecules and molecules with large dissociation

energies, the dissociation rate constant increases relatively slowly with excess energy, so the internal energy may exceed the energy required to dissociate into several dissociation channels. Thus, at high energy fluence the intensity controls the excess energy and the relative yields into each dissociation channel.

Frequency tuning below the resonant frequency causes the SF_6 quasi-continuum cross section to increase and the fraction of molecules excited to the quasi-continuum to decrease. Thus, frequency variations cause changes in the quantitative predictions for the laser intensity and energy fluence dependences of $\langle n \rangle$, or dissociation yield, and of excess energy with which molecules dissociate. Collisions can also cause changes in the quantitative predictons because collisions during the laser pulse can affect the fraction of molecules excited to the quasi-continuum. Collisions, even if absent during the laser pulse, can change the quasi-continuum population distribution, hence, altering the dissociation yield and the average excess energy after the laser pulse is over.

REFERENCES

1. D. M. Brenner, Chem. Phys. Lett. 57, 357 (1978).
2. P. A. Schulz, Aa. S. Sudbø, E. R. Grant, Y. R. Shen, and Y. T. Lee, "SF_6 Multiphoton Dissociation by a Molecular Beam Method", J. Chem. Phys. (to be published).
3. For reviews, see P. A. Schulz, Aa. S. Sudbø, D. J. Krajnovich, H. S. Kwok, Y. R. Shen, and Y. T. Lee, Ann. Rev. Phys. Chem. 1979. N. Bloembergen and E. Yablonovitch, Phys. Today 31(5), 23 (1978). V. S. Letokhov, Comments Atomic Mol. Phys. 8, 39 (1978).
4. Aa. S. Sudbø, P. A. Schulz, E. R. Grant, Y. R. Shen, and Y. T. Lee, J. Chem. Phys. 70, 912 (1979).
5. J. L. Lyman, J. Chem. Phys. 67, 1868 (1977).
6. E. R. Grant, P. A. Schulz, Aa. S. Sudbø, Y. R. Shen, and Y. T. Lee, Phys. Rev. Lett. 40, 1115 (1978).
7. M. Quack, J. Chem. Phys. 69, 1282 (1978).
8. W. Fuss, Chem. Phys. 36, 135 (1979).
9. J. G. Black, P. Kolodner, M. J. Schultz, E. Yablonovitch, and N. Bloembergen, Phys. Rev. A 19, 704 (1979).
10. Aa. S. Sudbø, P. A. Schulz, D. J. Krajnovich, Y. T. Lee, and Y. R. Shen, Opt. Lett. 4, 219 (1979).
11. D. F. Dever and E. Grunwald, J. Am. Chem. Soc. 98, 5055 (1976).
12. J. R. Ackerhalt and H. W. Galbraith, J. Chem. Phys. 69, 1200 (1978); Opt. Lett. 3, 109 (1978).

13. M. C. Gower and K. W. Billman, Opt. Commun. 20, 123 (1977).

14. J. L. Lyman and S. D. Rockwood, J. Appl. Phys. 47, 595 (1976).

15. P. Kolodner, C. Winterfeld, and E. Yablonovitch, Opt. Commun. 20, 119 (1977).

16. J. C. Stephenson, D. S. Ying, M. F. Goodman, and J. Stone, J. Chem. Phys. 70, 4496 (1979).

17. D. J. Krajnovich, A. Giardini-Guidoni, Aa. S. Sudbø, P. A. Schulz, Y. R. Shen, and Y. T. Lee, "Crossed Laser and Molecular Beam Study of Multiphoton Dissociation of C_2F_5Cl" presented at the European Physical Society Conference, Edinburgh, Scotland, September 1978.

18. R. B. Hall and A. Kaldor, J. Chem. Phys. 70, 4027 (1979).

Appendix A

Our RRKM computations have been performed using a computer program written by W. L. Hase and D. Bunker. In the initial calculations a dissociation energy of 77 kcal/mole was used; however, evidence has accumulated to show that the correct dissociation energy should be closer to 93 kcal/mole.[1] In the present calculation, we used a bond energy of 93 kcal/mole in the molecule. Fig. A1 shows the predicted RRKM rate constants for SF_6 and SF_5 as a function of excess energy.

A critical configuration is constructed by applying the minimum state density criterion. The density of states is calculated given the potential curve (assumed to be a Morse potential), vibrational frequencies and moments of inertia in the critical configuration (assumed to be functions of the reaction coordinate). The reaction coordinate is taken as the S-F internuclear bond distance. The vibrational frequencies in the critical configuration are 774, 642 (2), 948(2), and 481(7) cm^{-1} and two others which depended on the reaction coordinate. The assumed 481 cm^{-1} mode is the harmonic mean of all SF bending motions. All the other frequencies are SF stretches. One of the original 948 cm^{-1} stretch modes of the unexcited SF_6 disappears because the stretching is along the reaction coordinate. The SF bending modes are weakened in the critical configuration. An empirical formula which has been found useful in RRKM calculation for calculating frequencies of the softened bending modes in the critical configuration is:

$$\nu^{+}(r^{+}) = \nu^{0} \exp(-1.9\, r^{+}/r^{0})$$

where $r^0 = 1.56$ Å is the equilibrium bond distance and $\nu^0 = 481$ cm^{-1}

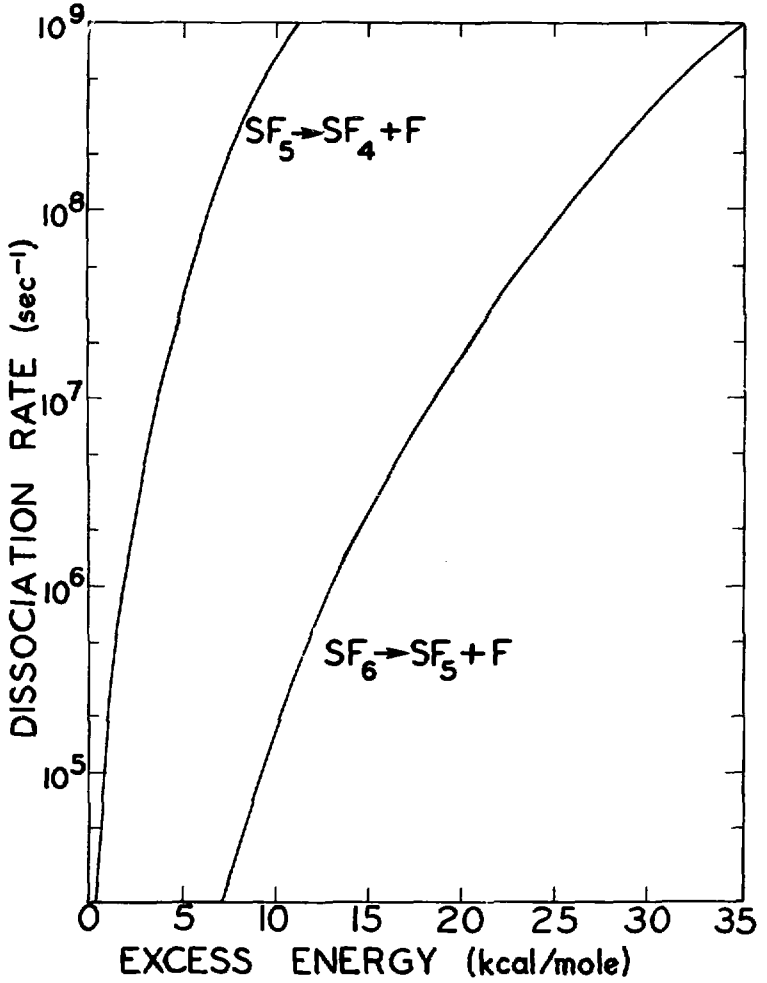

XBL 792-8353

Fig. A1. RRKM calculated rate constant using a dissociation energy of 93 kcal/mole for $SF_6 \rightarrow SF_5 + F$ and a dissociation energy of 51 kcal/mole for $SF_5 \rightarrow SF_4 + F$.

is the equilibrium frequency. The moments of inertia in the critical configuration were calculated in a straight-forward manner. The minimum density of states search results in a value of the reaction coordinate of 3.7 Å for a given excitation energy E^+ = 117 kcal/mole.

A similar RRKM calculation has also been performed on the $SF_5 \rightarrow SF_4 + F$ dissociation. In this RRKM calculation many guesses must be made since there is very little data (except for energetics) on the SF_5 molecule. The moments of inertia for the ground state are determined using an SF_5 geometry identical to SF_6 with one of the fluorines missing. We estimate the vibrational frequencies of SF_5 from known vibrational frequencies for SF_5Cl, SF_6, and SF_4 to be 932(?), 772(1), 642(2), 613(1), 522(3), and 344(3) cm^{-1}.

The structure of the SF_5 molecule in the critical configuration is assumed to be similar to SF_4 molecule with a SF bond stretch serving as the reaction coordinate. The frequencies in the critical configuration are 900(2), 750(1), 560(1), 510(2), 300(3), and 63(2) cm^{-1}. The rate constants determined from such an RRKM calculation are clearly much less reliable than those determined for the $SF_6 \rightarrow SF_5 + F$ dissociation. However, we expect that the calculated lifetimes for SF_5 are correct to within an order of magnitude.

REFERENCES

1. J. L. Lyman, J. Chem. Phys., 67, 1868 (1977).

Appendix B

The multiphoton dissociation experiments described in this thesis were carried out using the crossed laser-molecular beam apparatus described in Chapter II. The apparatus, shown in Fig. 1, consists of triple differential pumping of the molecular beam source, an interaction region where the laser crosses the molecular beam, and a rotatable triply differentially pumped detector that includes an electron bombardment ionizer and mass spectrometer.

Although the beam molecules are different from the multiphoton dissociation products, they produce many of the same ion fragments in 200 eV electron bombardment ionization. Therefore, the triple differential pumping of the molecular beam source, evident in Fig. 1, is necessary to reduce the background ion intensity when the detector is at small angles from the molecular beam. Within approximately 10° of the molecular beam direction, the detector ionizer can "see" effusion from the slit of the final differential pumping region of the molecular beam source. With triple differential pumping of the beam source, the slit in the final region is selected so that it does not collimate the beam, that is, the slit is large enough that all of the molecular beam passes through the slit. In this way the number density at the third slit is more than two order of magnitude smaller than the number density at a slit which collimates the molecular beam. Thus, the effusion from the slit and the background in the ionizer from this source is reduced by two orders of magnitude.

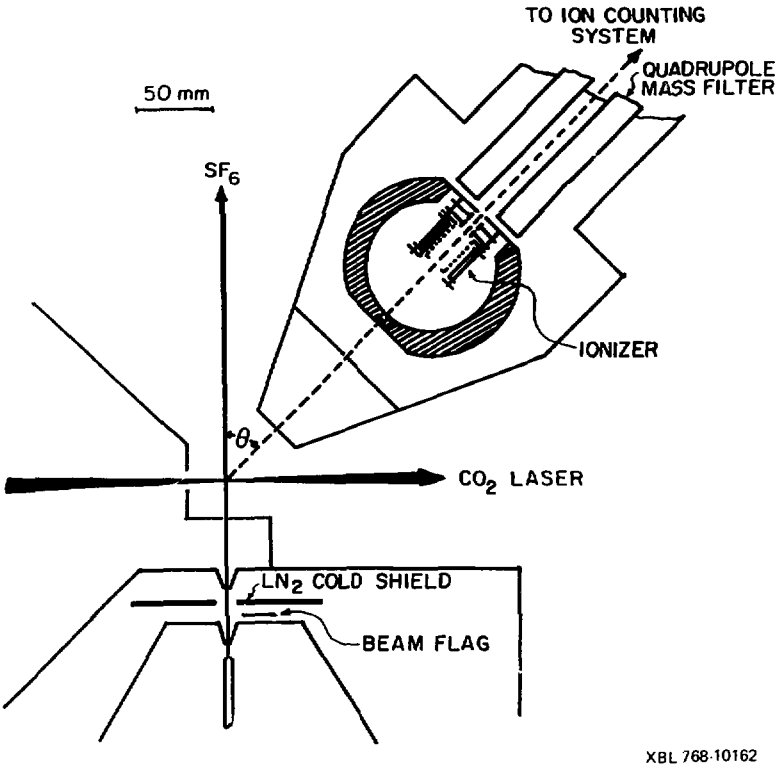

Fig. 1. Diagram of the molecular beam apparatus used for the study of SF_6 multiphoton dissociation.

However, in our molecular beam apparatus, the addition of a third differential pumping region does not decrease the background by the expected two orders of magnitude because elastic scattering of the molecular beam by the 5×10^{-7} residual gas in the main chamber is the major source of background at small angles from the molecular beam. The elastic scattering background is approximately ten times smaller than the background expected from use of only two differential pumping chambers, but is an order of magnitude larger than the effusive background from the slit of the third differential region.

Background can be reduced further by observing an ion mass that is prodigiously created from the multiphoton dissociation fragment, but not from the beam molecules. Therefore, the electron bombardment ion fragmentation ratios of the neutral multiphoton dissociation fragments are given in Table 1. The first column gives the molecular radical species produced in the dissociation deduced from the ion fragmentation ratios and the translational energy distributions. The parent molecules are given in the second column and can either be the beam molecules or their primary multiphoton dissociation products (e.g., SF_5 from SF_6 MPD and $CFCl_2$ from $CFCl_3$ MPD). The third column gives the ion fragment observed. The most abundant ion fragment is arbitrarily scaled to a value of 10. The random error in measurement of ion fragment ratios is approximately ±1. However, there are systematic errors that may be larger. One systematic error, the dependence of the ion fragment ratio on the electric quadrupole mass

Table 1. Fragmentation ratios obtained in 200 volt electron bombardment ionization of molecular radicals.

Neutral Fragment	Parent	Ion Fragments and Ratios
CF_3	CF_3Cl	$CF_2^+(10)$, $CF^+(4)$, $CF_3^+(0.8)$
	CF_3Br	$CF_2^+(10)$, $CF^+(4)$, $CF_3^+(0.8)$
	CF_3I	$CF_2^+(10)$, $CF^+(4)$, $CF_3^+(2.7)$
CF_2Cl	CF_2Cl_2	$CF_2^+(10)$, $CF_2Cl^+(9)$, $CF^+(7)$
CF_2Br	CF_2Br_2	$CF_2Br^+(10)$, $CF_2^+(2)$, $CF^+(2)$
$CFCl_2$	$CFCl_3$	$CFCl^+(10)$, $CFCl_2^+(6.5)$, $CF^+(3.5)$, $CCl^+(2.8)$, $CCl_2^+(2)$
$CFCl$	$CFCl_2$	$CFCl^+(10)$, $CF^+(5)$
	$CHFCl_2$	$CF^+(10)$, $CFCl^+(<3)$
CF_2	CHF_2Cl	$CF^+(10)$, $CF_2^+(5)$
C_2HCl_2	C_2HCl_3	$C_2HCl^+(10)$, $C_2HCl_2^+(10)$
C_2F_5	C_2F_5Cl	$CF_2^+(10)$, $CF_3^+(10)$, $CF^+(7)$, $C_2F_4^+(6)$
SF_5	SF_6	$SF_3^+(10)$, $SF_2^+(2)$
SF_4	SF_5	$SF_3^+(10)$, $SF_2^+(4.5)$
NF_2	N_2F_4	$NF^+(10)$, $NF_2^+(5)$, $F^+(0.7)$

filter settings is to a large extent avoided by operating the quadrupole at a low enough resolution that the ion intensity is saturated.

In order to understand the origin of the systematic errors, the analysis of the multiphoton dissociation of the members of the CF_3X series, where X=Cl, Br, I is considered. The fragments of the multiphoton dissociation were CF_3, detected in the mass spectrometer mainly as CF_2^+ and CF^+, both with identical velocity and angular distributions, and X with different distributions. The distributions of CF_3 and X were correlated by the conservation of linear momentum in the dissociation process. The ratios between the mass spectrometer signals of CF_3^+, CF_2^+, and CF^+ were determined for each of the three cases. The ratios were independent of laser energy fluence and the product translational energy (within the ±1 uncertainty). When the ion fragments come from the same CF_3 dissociation product, the ion fragment ratios should be the same. The CF_2^+:CF^+ ratio is the same in all three cases. However, the CF_3^+:CF^+ ion ratio changes from 0.8:10 for CF_3Cl and CF_3Br parent to 2.7:10 for CF_3I parent. Since up-excitation competes with dissociation to determine the excess energy when the molecules dissociate and CF_3I has the highest dissociation rate constant for a given excess energy, the nascent CF_3 and CF_3I should have the smallest amount of vibrational energy. The smaller amount of internal vibrational energy in CF_3 from CF_3I parent probably causes the small increased yield of CF_3^+.

A similar but more dramatic change in the ion fragment ratios is observed in the ionization of CFCl from both $CFCl_2$ and $CHFCl_2$ parents.

The CFCl formed in $CFCl_2$ multiphoton dissociation by atomic elimination should be vibrationally cold because the dissociation rate is huge even at internal energies just above the dissociation energy. CFCl formed in $CHFCl_2$ multiphoton dissociation by molecular elimination should be vibrationally hot, because the dissociation rate just above the dissociation energy is not so large and there is an energy barrier which is released in the dissociation. Part of this energy barrier probably appears as CFCl vibrational energy. Thus, increasing the vibrational energy in CF_3 and CFCl causes a decrease in the ion fragment ratio for the most massive (parent) ion fragment. The ion fragmentation dependence on vibrational energy is a large source of systematic errors and therefore Table 1 should be used as a not-too-accurate guide.

Appendix C

This appendix contains the computer program used for the model calculations described in Chapters 2 and 3. The comments in the program make it self-explanatory.

```
      PROGRAM TDMPA2 (INPUT,OUTPUT,TAPE5=INPUT,TAPE6=OUTPUT)
C
C TIME DEPENDENT MULTIPHOTON ABSORPTION - VERSION 2.
C THIS PROGRAM CALCULATES MPA BY INTEGRATION OF A SET OF RATE EQUATIONS.
C THE INTEGRATION OVER TIME IS DONE AT INTERVALS OF DT.  RECOMMENDED
C VALUES OF DT ARE BETWEEN .01 AND .001 NSEC.  THERE ARE 3 SUBROUTINES.
C A WORD ABOUT UNITS?
C TIME IN NANOSECONDS.        ENERGY IN KCAL.      RATE CONSTANTS IN GHZ.
C C POWER DENSITY IN MEGAWATTS/CM2.   CROSS SECTIONS IN 1.0E-19 CM2.
C
      COMMON DT
      DIMENSION TITLE(20),RTK(100),ABS(100),SE(100),POP(100),POPPRV(101)
      DIMENSION DISSON(100), POW(400)
      DIMENSION P(60),PPRV(61),RTK2(60),ABS2(60),SE2(60),DISS2(60)
      DATA CONST,NDIMN/.0144,100/
C CONST IS A CONVERSION CONSTANT NEEDED FOR THE VARIABLE C.
C
CARD 20A4.  TITLE
CARD 2I10,2F10.4.  NP,NTBP,DT,TMAX.
CARD 4I10.  LEVEL,LDISS,LEVE2,LDIS2.
CARD 8F10.4.  RTK.  LEVEL-LDISS+1 NUMBERS EXPECTED.
CARD 8F10.4.  RTK2.  LEVE2-LDIS2+1 NUMBERS EXPECTED.
CARD 2F10.4.  WHI,PKI.
CARD 4F10.4.  ABS(1),ABSF,ABS2(1),ABSF2.
CARD 110,3F10.4,I10,2F10.4.  NFREQ,EZERO,BETA,DE,NFREQ2,EZERO2,BETA2.
CARD 8F10.4. POW.  NF NUMBERS EXPECTED.
CARD F10.4.  ENRG
C
800   FORMAT (20A4)
801   FORMAT (2I10,2F10.4,I10)
802   FORMAT (I10,3F10.4,I10,2F10.4)
803   FORMAT (8F10.4)
804   FORMAT (4I10)
900   FORMAT (1H1,20A4)
901   FORMAT (* TIME INCREMENT =*,F5.3,* NSEC.*)
902   FORMAT (1H ,10F10.3)
903   FORMAT (*0THE LASER POWER IN MW/CM2.*/*POWER IS GIVEN AT INTERVALS
     1 OF*,F8.4,* NSEC.  TOTAL ENERGY =*,F6.2,* J/CM2*,35X,*ENERGY*)
904   FORMAT (*0PARAMETERS IN THE FIRST DISSOCIATION?*)
905   FORMAT (* MAXIMUM LEVEL =*,I3,* DISSOCIATIVE LEVEL =*I3,*(INCLUDIN
     1G LEVEL 0.)*)
906   FORMAT (*0PARAMETERS IN THE SECOND DISSOCIATION?*)
907   FORMAT (*0PARAMETERS OF EQUATION FOR POP(1).  GAMMA =*F5.2*DELTA =
     1*F5.1)
908   FORMAT (*0THE QUASI-CONTINUUM STARTS AT LEVEL*I2)
1     READ (5,800) TITLE
C
C NP NUMBER OF POWERS TO BE INPUT.
C NTBP NUMBER OF TIME INTERVALS TO THE OUTPUT OF THE POP. DISTRIBUTIONS.
C DT TIME INCREMENT FOR THE INTEGRATION.
C TMAX DURATION OF THE LASER PULSE.  TMAX/DT=NO. OF TIME INTERVALS.
C ALL VARIABLES BEGINNING WITH L ARE INTEGERS WHICH CORRESPONDTO AN
C ENERGY OF DE*LXXXX. THE SAME VARIABLE PRECEDED BY AN I, AS IN ILXXXX,
C IS JUST ILXXXX=LXXXX+1.  THIS IS TO GET RID OF THE PROBLEM THAT THE
C POPULATION AT 0 ENERGY RESIDES IN THE VARIABLE POP(1).
C ILEVEL IS THE NUMBER OF LEVELS INCLUDED IN THE FIRST DISSOCIATION.
C ILEVE2 IS THE NUMBER OF LEVELS INCLUDED IN THE SECONDARY DISSOCIATION.
C LDISS,LDIS2 CORRESPOND TO THE DISSOCIATION ENERGIES(1 AND 2), RESP.
C LUP IS THE LEVEL IN THE SECOND ABSORPTION BEYOND WHICH THER IS NO
C DECAY INTO HIGHER LEVELS OF THE SECOND MOLECULE FROM THE FIRST.
C LQC IS THE FIRST LEVEL OF THE QUASI-CONTINUUM
```

```
20      E = E+POW(I)
        E = E*TMAX/(NP*1000.)
C INITIAL POPULATION DISTRIBUTION.
        POP(1) = 1.
        POPPRV(1) = 1.
        POWMAX = 0.
C
C PRINT OUT THE ENERGY AND POWER DENSITIES OF THE LASER.
C ENRG TOTAL ENERGY DENSITY IN J/CM2 FOR NORMALIZING POWER DENSITY.
C E IS THE TOTAL ENERGY DENSITY OF THE LASER.
C
        READ (5,803) ENRG
        IF (ENRG .LE. 0.) STOP
        DO 30 I=1,NP
30      POW(I) = POW(I)*ENRG/E
        WRITE (6,903) (TMAX/NP),ENRG
        WRITE (6,902) (POW(I),I=1,INP)
        WRITE (6,908) LQC
        WRITE (6,907) WHI,PKI
        NNT = TMAX/DT
        WRITE (6,901) DT
C
C NOW DO THE INTEGRATION.  INCREMENT OVER TIME, AND FOR EACH TIME CALCU-
C LATE THE POPULATION DISTRIBUTIONWHICH RESIDES IN THE ARRAYS POP AND P.
C ABS,ABS2 ARE THE FULL ARRAY OF ABSORPTION CROSS SECTIONS.
C SE,SE2 ARE THE ARRAYS OF STIMULATED EMISSION CROSS SECTIONS FROM PREP.
C C A COEFFICIENT IN THE RATE EQUATIONS INVOLVING THE POWER DENSITY.
C  POPPRV IS THE PREVIOUS POPULATION DISTRIBUTIONFOR THE PRIMARY DISSOC.
C PPRV IS THE PREVIOUS POPULATION DISTRIBUTION FOR THE SECOND DISSOC.
C DISSON,DISS2 CONTAIN THE TOTAL DISSOCIATION YIELDS FROM EACH LEVEL.
C
        DO 100 I=1,NNT,NTBP
        CALL DISTR (ILEVEL,NDIMN,PCPPRV,I,ABS,SE)
        IF (LEVE2.NE.0) CALL DISTR  (ILEVE2,NDIMN,PPRV,I,ABS2,SE2)
        DO 90 J=1,NTBP
        TMP = ((I+J-2.)*NP/NNT)+1.
        ITMP = INT(TMP)
        TMP1 = TMP-ITMP
        POWER = TMP1*POW(ITMP+1)+(1.-TMP1)*POW(ITMP)
        IF (POWER.LE..00001) GO TO 90
        C=POWER*DT*CONST/DE
        IF (POWER.LE.POWMAX) GO TO 75
        POWMAX = POWER
        POP(1) = (1.-ERF(WHI*ALOG(POWER/PKI)))/2.
75      POP(ILQC) = POPPRV(ILQC)-POP(1)+PCPPRV(1)+C*(SE(ILQC)*POPPRV(IILQC
     1 )-ABS(ILQC)*POPPRV(ILQC))
        DO 80 K=IILQC,ILEVEL
        POP(K) = POPPRV(K)*(1.-DT*RTK(K))+C*(ABS(K-1)*POPPRV(K-1)+SE(K)*PO
     1PPRV(K+1)-(ABS(K)+SE(K-1))*POPPRV(K))
        DISSON(K) = DT*RTK(K)*PCP(K)+DISSON(K)
80      POPPRV(K-1) = POP(K-1)
        POPPRV(1) = POP(1)
        POPPRV(ILEVEL) = PCP(ILEVEL)
        IF (LEVE2.EQ.0) GO TO 90
C
C CALCULATE THE ABSORPTION FOR THE SECOND STEP.
C
        P(4) = PPRV(4)+C*(SE2(4)*PPPV(5)-ABS2(4)*PPPV(4))+POPPRV(4+LDISS)
     1*RTK(4+LDISS)*DT
        DO 85 L=5,LUP
        P(L) = PPRV(L)                    +C*(ABS2(L-1)*PPRV(L-1)+SE2(L)*PPRV(
     1L+1)-(ABS2(L)+SE2(L-1))*PPRV(L))+PCPPRV(L+LDISS)*DT*RTK(L+LDISS)
```

```
C
      READ (5,801) NP,NTBP,DT,TMAX,LQC
      ILQC = LQC+1
      IILQC = ILQC+1
      READ (5,804) LEVEL,LDISS,LEVE2,LDIS2
      ILDISS = LDISS+1
      ILEVEL = LEVEL+1
      LUP = ILEVEL-LDISS
      ILUP = LUP+1
      ILDIS2 = LDIS2+1
      ILEVE2 = LEVE2+1
      DO 5 I=1,LDISS
5     RTK(I) = 0.
      DO 6 I= 1,LDIS2
6     RTK2(I) = 0.
C
C 2 FOLLOWING A VARIABLE INDICATES THAT IT REFERS TO THE SECOND DISSCC.
C RTK,RTK2 RKKM RATE CONSTANTS FOR THE DISSOCIATION.
C WHI,PKI ARE PARAMETERS CONTROLLING THE INTENSITIES REQUIRED TO REACH
C THE QUASI-CONTINUUM.  WHI AFFECTS THE WIDTH OF THE INTENSITIES NEEDED.
C PKI IS THE INSENSITY WHERE HALF OF THE MOLECULES ARE IN THE QC.
C ABS(1),ABS2(1) FIRST ABSORPTION CROSS SECTION.
C ABSF,ABSF2. LAST ABSORPTION CROSS SECTION.
C DE ENERGY OF THE LASER PHOTON.
C NFREQ,NFREQ2 VIBRATIONAL DEGREES OF FREEDOM IN THE MOLECULE.
C EZERO,EZERO2 ZERO POINT ENRGY OF THE MOLECULE.
C BETA,BETA2  FREQUENCY DISPERSION PARAMETER. SEE ROBINSON AND HOLBROOK.
C POW IS THE ARRAY OF POWER DENSITIES OF THE LASER AS A FUNCTION OF TIME
C
      READ (5,803) (RTK(I),I=ILDISS,ILEVEL)
      IF (LEVE2.NE.0) READ (5,803) (RTK2(I),I=ILDIS2,ILEVE2)
      READ (5,803) WHI,PKI
      READ (5,803) ABS(1),ABSF,ABS2(1),ABSF2
      READ (5,802) NFREQ,EZERO,BETA,DE,NFREQ2,EZERO2,BETA2
      NP = NP+1
      READ (5,803) (POW(I),I=2,NP)
C
C THIS PROGRAM ASSUMES THAT FOR VERY SHORT LIFETIME STATES, MOLECULES AT
C TIME T DISSOCIATE AT TIME T+DT.
      DO 7 I=ILDISS,ILEVEL
7     IF (RTK(I)*DT.GT.1.) RTK(I)=1./DT
      DO 8 I=ILDIS2,ILEVE2
8     IF (RTK2(I)*DT.GT.1.) RTK2(I)=1./DT
C
C INITIALIZE AND SET THE ARRAYS NECESSARY.
C
      INP = NP+1
      POW(1) = 0.
      POW(NP+1) = 0.
      POW(NP+2) = 0.
10    WRITE (6,900) TITLE
      WRITE (6,904)
      WRITE (6,905) LEVEL,LDISS
      CALL PREP(ABS,ABSF,SE,LEVEL,NFREQ,EZERO,BETA,DE,POP,DISSON,POPPRV,
     1NDIMN)
      IF (LEVE2.EQ.0) GO TO 15
      WRITE (6,906)
      WRITE (6,905) LEVE2,LDIS2
      CALL PREP(ABS2,ABSF2,SE2,LEVE2,NFREQ2,EZERO2,BETA2,DE,P,DISS2,PPRV
     1,NDIMN)
15    E = 0.
      DO 20 I=1,NP
```

```
85    PPRV(L-1)= P(L-1)
      DO 86 L=ILUP,ILEVE2
      P(L) = PPRV(L)*(1.-DT*RTK2(L))+C*(ABS2(L-1)*PPRV(L-1)+SE2(L)*PPRV(
     1L+1)-(ABS2(L)+SE2(L-1))*PPRV(L))
      DISS2(L) = DT*RTK2(L)*P(L)+DISS2(L)
86    PPRV(L-1) = P(L-1)
      PPRV(ILEVE2) = P(ILEVE2)
90    CONTINUE
100   CONTINUE
C
C CONCLUDE THE PROGRAM BY PRINTING OUT THE DESIRED INFORMATION.
C
      CALL DISTR (LEVEL,NDIMN,PCP,I,ABS,SE)
      IF (ILEVE2.NE.0) CALL DISTR  (ILEVE2,NDIMN,P,I,ABS2,SE2)
      CALL CONCL (LOISS,RTK,DISSCA,PCP,NDIMN,ILEVEL)
      IF (LEVE2.NE.0) CALL CONCL(LOISZ,RTK2,DISS2,P,NDIMN,ILEVE2)
      GO TO 10
      END



      SUBROUTINE PREP(ABS,ABSF,SE,LEVEL,NFREQ,EZERO,BETA,DE,A,B,C,N)
C
C PREP PREPARES FOR THE REST OF THE PROGRAM BY INITIALIZING ARRAYS AND
C CALCULATING THE CROSS SECTIONS FOR ABSORPTION AND STIMULATED EMISSION.
C ABS AND SE ARE RELATED BY THE RATIO OF THE DENSITY OF STATES AS
C CALCULATED BY THE WHITTEN-RABINOVITCH APPROXIMATION INCLUDING ROTATION
C RDS IS THE RATIO OF THE DENSITY OF STATES.
C
      DIMENSION ABS(N),SE(N),RDS(100),G(100),A(N),B(N),C(101)
902   FORMAT (1H 10F10.5)
904   FORMAT (*0RATIO OF THE DENSITY OF STATES BETWEEN ADJACENT LEVELS*)
905   FORMAT (*0ABSORPTION CROSS SECTION IN 1.0E-19 CM2.*)
      DO 5 I=1,N
      A(I)=0.
      B(I)=0.
5     C(I)=0.
      C(N+1) = 0.
      G(1) = .5
      DO 8 I=1,LEVEL
      ABS(I+1)= ABS(1)*(ABSF/ABS(1))**(FLOAT(I)/(LEVEL-1.))
      EPR = I*DE/EZERO
      IF (EPR.GE.1.) GO TO 6
      W=1./(5.*EPR+2.73*SQRT(EPR)+3.51)
      WPR = -(5.+1.365/SQRT(EPR))*W*W
      GO TO 7
6     W = EXP(-2.4191*EPR**0.25)
      WPR = -0.60478*W*EPR**(-0.75)
7     G(I+1) = (EPR+1.-BETA*W)**(NFREQ-1)  *(1.-BETA*WPR)
8     RDS(I) = G(I)/G(I+1)
      DO 10 I=1,LEVEL
10    SE(I) = ABS(I)*RDS(I)
      ABS(LEVEL+1) = 0.
      SE(LEVEL+1) = 0.
      WRITE (6,904)
      WRITE (6,902) (RDS(I),I=1,LEVEL)
      WRITE (6,905)
      WRITE (6,902) (ABS(I),I=1,LEVEL)
      RETURN
      END
```

```
      SUBROUTINE DISTR (ILEVEL,N,POP,I,ABS,SE)
C
C DISTR OUTPUT THE POPULATION DISTRIBUTION WHICH RESIDES IN POP.
C SUM CONTAINS THE TOTAL POPULATION IN THE MOLECULE(UNDISSOCIATED.)
C AVG CONTAINS THE AVERAGE NUMBER OF PHOTONS ABSORBED.
C
      COMMON DT
      DIMENSION POP(N),ABS(N),SE(N)
901   FORMAT (*0POPULATION DISTRIBUTION AFTER*,F8.2,* NSEC. SUM =*,F5.6,
     1* AVERAGE EXCITATION =*F6.2* CROSS SECTION =*F6.2)
902   FORMAT (1H ,10F10.7)
      AVG = 0.
      SUM=0.
      CS = ABS(1)*POP(1)
      DO 63 K=2,ILEVEL
63    CS = (ABS(K)-SE(K-1))*POP(K)+CS
      DO 70 K=1,ILEVEL
      AVG = AVG+(K-1.)*POP(K)
70    SUM= SUM+POP(K)
      IF (SUM.LE.1.E-8) SUM=1.
      WRITE (6,901) DT*(I-1),SUM,AVG/SUM,CS/SUM
      WRITE (6,902) (POP(K),K=1,ILEVEL)
      RETURN
      END



      SUBROUTINE CONCL(LDISS,RTK,DISSON,POP,N,ILEVEL)
C
C CONCL CONCLUDES THE PROGRAM BY PRINTING THE DISSOCIATION YIELDS AT THE
C END OF THE PULSE.
C
      DIMENSION RTK(N),DISSON(N),POP(N)
906   FORMAT (*1DISSOCIATION YIELD*/5HLEVEL,8X,13HRATE CONSTANT,7X,8HYIE
     1LD ON,10X,9HYIELD OFF,10X,11HTOTAL YIELD)
907   FORMAT (1H0,I4,8X,F10.5,10X,F8.5,11X,F8.5,11X,F8.5)
      TDON = 0.
      TDOFF = 0.
      WRITE (6,906)
      ILDISS = LDISS+1
      DO 120 I=ILDISS,ILEVEL
      WRITE (6,907) I-LDISS,RTK(I),DISSON(I),POP(I),POP(I)*DISSON(I)
      TDON = TDON + DISSON(I)
120   TDOFF = TDOFF+POP(I)
      I=0
      A=0.
      WRITE (6,907) I,A,TDON,TDOFF,TDON+TDOFF
      RETURN
      END
```

U.S. GPO: 1979 - 698-169/F89